UNIVERSITY OF OKLAHOMA

GRADUATE COLLEGE

A SEASONAL TO SUBSEASONAL EXAMINATION OF SYNOPTIC AND LOCAL DRIVERS OF FLASH DROUGHT

A DISSERTATION

SUBMITTED TO THE GRADUATE FACULTY

in partial fulfillment of the requirements for the Degree of

DOCTOR OF PHILOSOPHY

By

Daniel Mesheske

Norman, Oklahoma 2024

A SEASONAL TO SUBSEASONAL EXAMINATION OF SYNOPTIC AND LOCAL DRIVERS OF FLASH DROUGHT

A DISSERTATION APPROVED FOR THE

SCHOOL OF CIVIL ENGINEERING AND ENVIRONMENTAL SCIENCE

BY THE COMMITTEE CONSISTING OF

Dr. Pierre Kirstetter, Chair

Dr. Jefferey Basara

Dr. Yang Hong

Dr. Xianming Xiao

Dr. Randall Kolar

Acknowledgements

The completion of this dissertation would not have been possible without the support of many incredible people in my life. First, I would like to thank my parents and brother for the encouragement to leave a stable career in the pursuit of graduate education, and their continued support throughout the pursuit of a PhD.

Next, I would like to thank Dr. Jeff Basara for taking a chance on me despite my "untraditional" path. His mentorship has been invaluable to me becoming the researcher that I have become. As both official and unofficial advisor he has taught me to be a better writer, scientist, speaker, teacher, and overall human being.

Despite not being on my committee Dr. Jason Furtado and Dr. Jordan Christian were instrumental in the completion of this work. Jason and Jordan spent countless hours with me fostering my research, computer science and writing skills. Also thank you to Dr. Paul Flanagan, as former CHEWe members both Jordan and Paul's research created a base for me to build upon in this dissertation. I would also like to thank the current members of CHEWe for their support and companionship through both good and the bad. Thank you to Taylor Grace, Ben Fellman, Henry Olayiwola, and Noah Brauer, who have always made time to discuss research and ideas with me and coauthor manuscripts. I fully expect them all to make an impact with their own work going forward. As Jeff would say "Iron sharpens iron".

I would like to thank my other committee members Dr. Yang Hong, Dr. Xianming Xiao, and Dr. Randy Kolar. Through classes or the composition of this dissertation all three have been invaluable to my completion. I would also especially like to thank Dr. Pierre Kirstetter for his willingness to step in and take over the committee at the last moment. His input, mentorship, and advising over the last few months of this work was immeasurable.

Finally, I would like to thank my partner Karianne for standing by me during this process and continuing to push me during the hard times. I cannot express how important your support has been, and Sophie, your cool too. I guess.

Table of Contents

ABSTRACT:

Flash drought is the rapid intensification of drought like conditions. Initiated by meteorological processes that quickly desiccate soil they can be devastating to agriculture and local ecosystems. Flash droughts are driven by a complex interaction of many terrestrial and atmospheric processes making prediction challenging. The prediction of future flash drought events will require a better understanding of these complex interactions. In particular, synoptic scale processes that lead to changes in evaporative stress are poorly understood, and little is known as to how they impact the local processes. To better predict flash drought both remote teleconnections and the effects of evaporative stress on local terrestrial conditions must be identified. Additionally, the temporal lag from remote drivers to flash drought development needs to be quantified.

Using current datasets, multiple methods focusing on synoptic and local spatial scales from seasonal to sub seasonal temporal scales were used to increase our understanding of conditions that drive flash drought. Seasonal atmospheric variables were used to identify areas in Europe primed for agricultural flash drought development in a later season. Additionally, sea surface teleconnections and synoptic scale atmospheric processes were examined before and during flash drought development to identify remote drivers. Lastly, the identified remote drivers were mathematically and statistically assessed for both their covariance with evaporative stress and their correlation with changes in evaporative stress in the Central US.

Chapter 1: Introduction

Climate change and continued population growth will have significant impacts on global water security. The frequency of hydrologic natural hazards such as drought are expected to increase as anthropogenic warming continues (Gudmundsson and Seneviratne, 2016; Christian et al., 2021). Higher temperatures and more frequent heatwaves will increase the risk of both drought occurrence (Wen et al., 2023) and location. The Food and Agriculture Organization of the UN attributes $250-300 billion in economic losses annually to drought and expects these losses to increase (Zhang et al., 2022). First identified in 2002 (Svoboda et al., 2002) flash drought is the rapid intensification of drought conditions. Flash drought is an atmospherically driven, meteorological drought that can quickly progress into agricultural or possibly hydrological drought (Christian et al., 2024). This rapid change can lead to detrimental impacts across a variety of sectors including agriculture, water security, human health, and natural ecosystems (Wilhite et al., 2007; Basara et al., 2019; Christian et al., 2019, Wen et al., 2023, Christian et al., 2024).

Precipitation deficits are the primary driver of all drought events. However, the rapid evolution of flash drought is accelerated by more than lack of precipitation alone. Often, the evaporative stress is recognized as the primary metric that drives flash drought, particularly on a regional scale (Christian et al., 2019b). Soil moisture declines or deficits are often used to characterize flash droughts (Osman et al., 2022; Yuan et al., 2019) as they can easily identify and track propagation of flash drought within the terrestrial ecosystem. However, changes in soil moisture represent the nexus of meteorological and agricultural drought, and not the

meteorological conditions that drive the changes in soil moisture conditions. Measures of evaporative stress such as the Rapid Change Index (Otkin et al., 2014) or the Standardized Evaporative Stress Ratio (Christian et al., 2021;2019b) are robust as they account for several near surface state variables that influence both land and atmosphere at various temporal scales.

While rapid onset is a consensus criterion for flash drought development, a universal definition (Otkin et al., 2018; Lisonbee et al., 2021) has been elusive. A such, flash droughts have been defined by rapid change, duration, or by indicators such as evaporation, soil moisture, precipitation, temperature, or changes to the United States (US) Drought Monitor (Svoboda et el. 2002). The disagreement over definitions can be attributed, in part, to the vast range of both regional and synoptic scale drivers that can influence the development of flash drought. At the same time, the combination of synoptic and regional drivers, and limitations to a general framework to identify flash drought hinders our ability to effectively monitor and predict its propagation (Otkin, 2022; Lisonbee et al., 2022).

Attempts to predict flash drought accurately and reliably have been elusive (Otkin et al., 2022). Beyond the influence of multi-scale processes, the temporal component of flash drought development is poorly understood. Again, disagreements exist on what duration constitutes a flash drought, some are defined by their short duration from 5- days to weeks (Lisonbee et al., 2022; Mo and Lettenmaier, 2016). However, at the shortest time scales (days) it can be difficult to differentiate between a flash drought and a dry spell without including rate of intensification. Further, most researchers consider flash drought to be a subseasonal to seasonal process; a temporal span considerably longer than 5 days. Thus, the rapid intensification period of flash drought conditions can be considered the “flash”. As such, drought conditions may exist before

or persist after the “flash” and possibly transition into longer term droughts such as the case of the 2012 US drought (Otkin et al., 2018b).

This seasonal to subseasonal period that flash droughts occur can be extremely difficult to forecast due to contributions from atmospheric, terrestrial, and oceanic drivers. Current weather forecasting heavily relies on data assimilation and numerical weather prediction to assess the current state of the atmosphere and then predict its evolution respectively (Weyn et al., 2021). Propagation of numerical inaccuracies can make these models ineffective at longer scales of 2 weeks to 2 months. Thus, other methods have been developed and utilized to predict flash drought including using forecasts as a precursor for predicting drought hazards (Richardson et al., 2021), statistical models, and machine learning (Zhang et al., 2023), all of which have advantages and disadvantages.

The chaotic nature of the atmosphere and climate system in combination with differing spatial and temporal scales of land, atmosphere, and ocean processes that all lead to flash drought create a prediction challenge (Ma and Yuan, 2023; Chen et al., 2020). Existing drought forecasting tools do not provide adequate early warning (Otkin et al., 2022). This may be in part to research focusing in on one hydrometeorological variable to address a problem caused by the joint effect of several systems (Wen et al., 2023). Pendergrass et al., (2020) noted, “A better understanding of flash droughts requires more in-depth research on relevant compound and cascading physical processes that can trigger or increase the likelihood of a flash drought. These include relationships among soil moisture, land–atmosphere interactions, their connections to large-scale meteorological conditions (and precursor conditions), and how these are forced by remote SST patterns and influenced by internal atmospheric variability”. Understanding these

connections and processes are a necessary foundation for any flash drought specific predictive model. Locally, feedbacks between evapotranspiration, temperature, and soil moisture that cascade during flash drought development have been well documented (Seneviratne et al., 2010). However, examination of these feedbacks on seasonal to subseasonal temporal scales has not. Increased understanding of the influences of temperature and evaporative stress inter-seasonally can raise awareness of initial conditions of flash drought development and may show utility for prediction.

Synoptically, slow moving or stalled high atmospheric ridges have been linked with flash drought development (PaiMazdur & Done, 2016; Ford & Labosier 2017; Basara et al., 2019; Bolles et al., 2021; Jong et al., 2022; Kautz et al., 2022). Ridging causes the subsidence of warm dry air that can desiccate the land surface. The larger atmospheric patterns, such as geopotential heights and zonal winds that slow ridges and divert moisture during flash drought are less understood. The North Central Pacific has been shown as an area of generation of Rossby wave packets that lead to ridges over the Central US (Jong et al., 2022), but what causes this generation and the atmospheric patterns that cause the packets to slow, or stall is not explained.

Cyclic SST oscillations have been shown to influence moisture patterns (Rasmusson & Carpenter, 1982; Flanagan et al., 2018; 2019) and drought in the US (Lesinger & Tian, 2022). However specific SST anomaly patterns that influence flash drought development and their influence on pressure heights and zonal winds have not been studied.

This dissertation will examine remote SST and atmospheric teleconnections, increase the scientific understanding of the processes, both remote and local, and build a base of knowledge to support increased prediction of Central US flash drought development. As such,

the hypothesis of this dissertation is that the current suite of environmental datasets is sufficient to 1) quantify local land-atmosphere interactions that drive flash drought through time to identify areas primed for flash drought, 2) determine the relationships between local and synoptic scale processes both before and during the development of flash drought, and 3) identify the patterns that create regional flash droughts and examine the lags between synoptic scale processes and local effects.

The following chapters 2 through 5 will address this hypothesis and goal. Chapter 2 will assess the ability to use average seasonal temperatures or evaporative stress to identify areas primed for flash drought development. The Standardized Evaporative Stress Ratio (Christian et al., 2021;2019b) and 2-meter temperature will be regressed across a seasonal time lag with root zone soil moisture, with soil moisture acting as a proxy for agricultural flash drought. Chapter 3 will identify both larger teleconnections and regional drivers that contribute to early growing season flash drought formation. Synoptic scale composites of Sea Surface Temperature, 500 and 250 mb Geopotential Heights, 250 mb U and V winds, and Temperature are investigated for both an antecedent period of 30 days before flash drought onset and a development period of 30 days after the start of rapid intensification. The same investigation will be conducted on a regional scale for two flash drought prone regions using Precipitation, Soil Moisture, and Vegetation Densities. In Chapter 4 the composites created are compared through Empirical Orthogonal Function analysis to assess the validity of the patterns identified in Chapter 3 and to quantify the temporal lag between larger ocean and atmospheric processes and regional impacts in the flash drought prone areas. Finally, Chapter 5 will provide an overarching synopsis, a discussion, and key findings.

Chapter 2: Using Seasonal Evaporative Stress Across Europe to Identify Areas Primed for Agricultural Flash Drought

2.1 Introduction:

Population growth and impacts due to climate change are increasing the importance of monitoring and predicting water resources. Continued anthropogenic warming is increasing the likelihood of drought (Gudmundsson and Seneviratne, 2016) with diverse regional and seasonal impacts on soil moisture availability (Samaniego et al., 2018). Drought can decimate agricultural regions and cause significant financial damages (Wilhite et al. 2007) with further impacts to surface and groundwater availability, recreation, human health, wildfires, and ecosystems (Basara et al., 2013, Christian et al., 2019b). Drought losses across Europe are estimated at 9 billion EUR annually with most of the damage in the agricultural sector (Naumann et al., 2021), and hydroclimate reconstructions show that the recent multi-year European droughts are unprecedented historically (Büntgen et al., 2021; Luterbacher et al., 2004). Climatologically, 2015 was the hottest and driest summer in the last 50 years (Ionita et al., 2015; Hoy et al., 2016) and, as warming continues, extreme drought and heat waves across Central Europe are expected to increase (Haskins 2022; Rakovec et al., 2022; Hari et al., 2020; Samaniego et al.; 2018, Bador et al., 2016a; Russo et al., 2014).

Despite significant impacts, drought often receives low public interest compared to other hydrometeorological disasters such as floods (Orth et al., 2022). Typically, drought has been identified according to three main physical types (Wilhite and Glantz, 1985): (1) *meteorological,*

consisting of a lack of precipitation and increased atmospheric evaporative demand (Spinoni et al., 2019; Stagge et al., 2015), (2) *agricultural,* with longer-term impacts of soil moisture and its effect on vegetative stress (Tian et al., 2018; Zhang et al., 2018; Lui et al., 2016; Geng et al., 2016), and (3) *hydrological,* with decreased discharge rates of surface water and depleted groundwater (Barker et al., 2016, Wada et al., 2013). First identified in 2002 (Svoboda et al., 2002; Lisonbee et al. 2022), flash drought is an acceleration of meteorological drought conditions into agricultural drought. Often defined as the rapid intensification of drought-like conditions (Otkin et al., 2018b; Christian et al., 2019b), flash drought is caused by desiccation of the terrestrial surface and is often driven by anomalous upper tropospheric ridging (Ford and Labosier, 2017; Christian et al., 2020) associated with blocking patterns (Rex 1950). Atmospheric blocking inhibits precipitation, increases temperature, and is often linked with compound drought and heat wave events (Kautz et al., 2022; Christian et al., 2020). While all droughts result from a precipitation deficit, the rapid progression of flash drought is accelerated through other drivers. Reduced precipitation in combination with increased temperatures lead to increased evaporative stress from the near surface atmosphere and recent studies have noted that the occurrence of flash drought will increase across Europe in the coming decades (Christian et al. 2023; Yuan et al. 2023).

The relationship between soil moisture, evaporative stress, and temperature is complex with feedbacks that can increase terrestrial warming (Seneviratne et al., 2010, Vogel et al., 2018). Via evapotranspiration (ET), soil moisture can be a source of water for the atmosphere (Seneviratne et al., 2010), with transpiration acting as the largest contributor to total land ET volumes (Dirmeyer et al., 2006, Lawrence et al., 2007) and can return up to 60% of precipitation that falls on land to the atmosphere (Oki and Kanae 2006). Lack of soil moisture can suppress

ET leading to increased temperatures (Lakshmi et al., 2004, Seneviratne et al., 2006) via restricted evaporative cooling (Donat et al., 2017). This is dramatically evident in European extreme heat waves which show strong moisture-temperature coupling (Lui et al., 2020) and feature pre-existing negative soil moisture anomalies (Bador et al., 2016b; Miralles et al., 2014). Combined drought and heatwave events are common, representing 30-40 percent of all hydrometeorological extremes (Orth et al., 2022), and future simulations point to a 5 to 8-fold increase in combined events in Central Europe and the Mediterranean, resulting from higher global temperatures (Mukherjee et al., 2022b). Heat waves often amplify drought effects on crop yields yet receive the lowest amount of hydrometeorological scientific scrutiny (Orth et al., 2022).

Soil moisture levels can dictate ET magnitudes and influence interannual variability of gross primary product (Stocker et al., 2019). Regional decreases in soil moisture during seasons vital to plant development (Samaniego et al., 2018) are coinciding with ecosystems becoming more vulnerable to water availability (Li et al., 2022). Vegetative response time to water scarcity is suggesting a stronger susceptibility to drought (Jiao et al., 2021) that varies in different land cover types. Soil moisture depletes faster in agricultural areas like croplands or grasslands than forests (Liu et al., 2020) making them more vulnerable to flash droughts (Yao et al., 2022). Rapid development of drought can be common, with roughly 40% of droughts in Spain considered rapid (Noguera et al., 2020) and between 1950 and 2019 flash drought frequency and spatial extent in Europe have greatly increased during the growing season (Shah et al., 2022).

The interaction between atmospheric evaporative stress and soil moisture conditions that yield flash drought can be viewed as the nexus of meteorological and agricultural droughts.

Identification of areas that are primed for flash drought development could allow stakeholders in the agriculture and water management sectors to better prepare for these extreme events. As such, this analysis examines (1) the seasonal relationship between temperature and root zone soil moisture across Europe, (2) the relationship between seasonal evaporative stress and soil moisture, (3) introduce seasonal lags to examine these relationships at inter-seasonal time scales, (4) use temperature and evaporative stress in multiple variable regression with RZSM to identify the larger driver of subsequent seasonal RZSM levels, and (5) using RZSM deficits as a proxy measurement for agricultural flash drought the results of these regressions will be compared to known flash drought events to assess the validity of the regression results.

2.2 Methods:

This study utilized the Modern-Era Retrospective analysis for Research and Applications, Version 2 (MERRA-2) reanalysis archive maintained by National Astronautics and Space Administration (NASA). The MERRA2 data is a gridded dataset with a resolution of 0.5° latitude x 0.625° longitude that ranges from 1980 – present. For this study we used the daily mean values for the period of January 1980 through December 2020 for each grid point for the continent of Europe including the following variables: 2-meter Temperature, u and v wind, radiation, pressure, evapotranspiration, and root zone soil moisture. The domain of the study area spans 30°-75°N and 26.875°- 65°N and includes a multitude of climate types.

The Standardized Evaporative Stress Ratio (SESR; Christian, et al. 2021; 2019b) was used to quantify evaporative stress. SESR is the standardized form of the Evaporative Stress Ratio (ESR); the ratio of actual Evapotranspiration (ET) to Potential Evapotranspiration (PET).

The ESR varies on a scale of 0 to 1 where 0 indicates that atmospheric demand is high and there is little moisture to meet it. Values closer to 1 indicate that demand is being met by available water (Christian et al., 2019b). The standardization process removes the mean and divides by the standard deviation creating a series of standardized anomaly values that typically range between 3 and -3. These anomalies measure deviation from the mean and offer a more robust metric than the ESR alone. For this study, PET was calculated via the Penman-Monteith FAO equation (Equation 2.1; Allen et al., 1998), using 2-m wind speed (U_2), net solar radiation at the crop surface (R_n), temperature (T), soil heat flux density (G), saturation vapor pressure deficit (e_s), vapor pressure (e_a), the slope vapor pressure curve (Δ), and the psychrometric constant (γ).

$$\boldsymbol{ET_o} = \frac{\mathbf{0.408}\Delta(\boldsymbol{R_n}-\boldsymbol{G})+\boldsymbol{\gamma}\frac{\mathbf{900}}{\boldsymbol{T}+\mathbf{273}}\boldsymbol{u_2}(\boldsymbol{e_s}-\boldsymbol{e_a})}{\Delta+\boldsymbol{\gamma}(\mathbf{1}+\mathbf{0.34}\boldsymbol{u_2})} \quad 2.1)$$

Next, at each grid point ESR was computed by dividing ET by PET and SESR was calculated by removing the mean and dividing by the standard deviation of the ESR ratios consistent with Christian et al (2021; 2019b; Equation 2.2). SESR values were validated via comparison to previously calculated and validated SESR values (Christian et al., 2019a).

$$\boldsymbol{SESR_{ijp}} = \frac{\boldsymbol{ESR_{ijp}}-\overline{\boldsymbol{ESR_{ijp}}}}{\boldsymbol{\sigma ESR_{ijp}}} \quad 2.2)$$

The daily mean 2-m temperature (T) data for the months of March, April, and May (MAM), June, July, and August (JJA), and September, October, and November (SON) were selected and averaged to create a single seasonal-mean value for each spring (MAM), summer (JJA), and fall (SON) season from 1980 to 2020 (i.e., 41 values per season). Similarly, SESR and Root Zone Soil Moisture (RZSM) data values were processed in the same manner. For each

resulting set of values, the linear trend was removed through least-squares fitting, and the detrended values were standardized. Linear regression analysis was performed between concurrent season temperature values and MERRA 2 RZSM throughout the domain and as a function of season. Pearson correlations (Everitt 2010) were calculated on a grid point basis for the entire study area. The same regression and correlation analysis was performed using SESR and RZSM, for all three time periods. We then performed seasonal lag regression to examine potential lead/lag relationships between variables. Finally, a multivariable regression was performed on all three variable sets to identify the strongest drivers.

Statistical significance testing was conducted using a 2-tailed *t*-test with $N = 41$ degrees of freedom. Statistical significance tests conducted on the correlation coefficients are done against a null hypothesis of $r = 0$ between the variables.

2.3 Results:

2.3.1 Climatology – Concurrent season relationships of T, SESR, and RZSM

Regressions of mean 2-m T with RZSM (Figs. 2.1a-c) yield a negative relationship that varies spatially across Europe between seasons. These negative correlations reinforce the known relationship that increases in T result in decreases of RZSM. The stronger negative correlations and areas of focused statistical significance (the overlaid stipple) are localized in regions that have warmer temperatures during the respective seasons.

The strongest correlations during the spring are in the southern areas of the continent reaching a minimum value of -0.77. These southern areas also show the most statistical

significance except for areas near the northern coasts. The reduced correlation in the north is the result of cooler temperatures later in the MAM season. Cooler temperatures can inhibit ET and allow soils to maintain larger moisture levels. The areas of increased significance along the northern coasts do not exhibit decreased correlation values despite the high t-scores. These areas are subject to the Gulf Stream which would affect localized T and ET

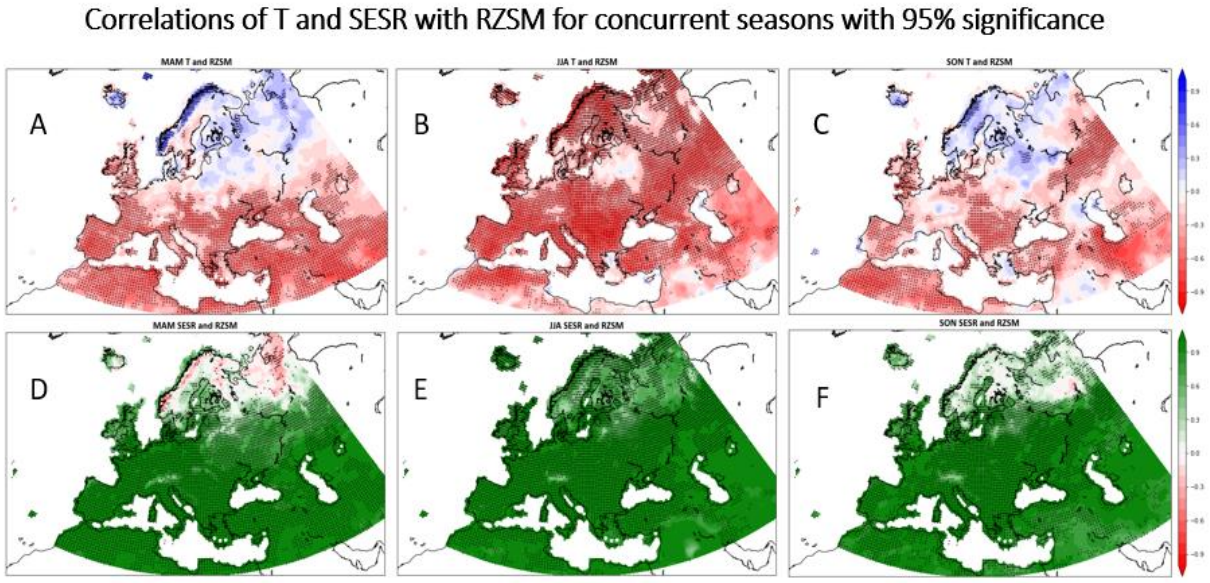

Figure 2.1: Correlations for seasonal regression of T and RZSM for a.) March, April, and May (MAM), b.) June, July, and August (JJA), and c.) September, October, and November (SON). Correlations of T and SESR for d.) MAM, e.) JJA, and f.) SON. All plots are overlaid with a stipple at grid points where the correlations exceeded the 95% confidence threshold.

During the boreal summer (Fig. 2.1b), higher negative correlations occurred in southern and inland localities over Europe. On a continental scale, few areas lack a significant relationship, and the continental average correlation is -0.53. There is an anomalous area in the

Baltics, Belarus, and Northwest Russia where the T and RZSM relationship holds little agreement.

Correlations during the boreal fall begin to decline due to cooler seasonal average temperatures (Fig. 2.1c) yet a few areas yield significance accompanied by decreased correlation values. Most of these locations reside further south, however, the southern portion of continent does not show as comprehensive coverage as in the spring (Fig. 2.1a). Finally, there is an additional area of strong correlation in Central Russia near the Urals.

Regardless of season, in regions south of approximately 55°N, correlations between SESR and RZSM are extremely strong (Fig. 2. d-f). These results confirm the influence that SESR, as a measure of evaporative stress, has on RZSM. It is notable that the relationship is consistent throughout most of the continent regardless of regional differences in climate and soil properties. Like other figures, there is less correlation in the northern regions that are more pronounced in the spring and fall.

2.3.2 – Inter-seasonal relationships of T, SESR, and RZSM

Figures 2.2 a and b show the correlations for T and RZSM when a one-season lag is applied. Correlations between MAM T and JJA RZSM (Fig. 2.2a) are not as strong as those of the concurrent JJA season regression (Fig. 2.1b). Regional areas still exhibit a strong negative correlation but are not as widespread. However, statistical significance is more widespread than that of the MAM concurrent plot. The variation is likely a result of regional climate, soil type, and ecosystem variations, but in regions with strong relationships, MAM or JJA T may be used to infer the following seasons soil moisture levels. While the correlations are not as strong when

lag is introduced, the statistical significance suggests that these relationships are still relevant on a seasonal temporal scale.

Unlike the spring and fall results from Figure 2.1, both the spring to summer and summer to fall analyses display regions of higher correlations and significance throughout much of Scandinavia. These signals appear despite the cooler Ts affecting the MAM and SON mean temperatures. The JJA to SON plot also exhibits a northward shift of higher correlations and significance indicating that JJA temperatures will have more influence on RZSM in far northern Europe.

The analysis of seasonal lag focused on the regression of evaporative stress and soil moisture displays a number of critical results (Fig. 2.2c-d). For example, the overall inter-seasonal relationship between SESR and RZSM exhibits as much significance as that of the concurrent season regression. While the correlations vary more regionally than that of the concurrent season JJA plot (Fig. 2.1e), the vast area that is significant covers much of the continent. Like Fig. 2.2b, the higher correlations shift to the north in the summer to fall regression.

The increased statistical confidence of the lag regression between evaporative stress and soil moisture may represent the temporally driven link between evaporative stress and ET. The seasonal mean values are likely too long of a period to accurately record this relationship. However, areas of high correlation indicate a direct seasonal impact of evaporative stress on RZSM. This correlation with the increased significance indicates that increased levels of evaporative stress is a predictand of soil moisture depletion during the following season.

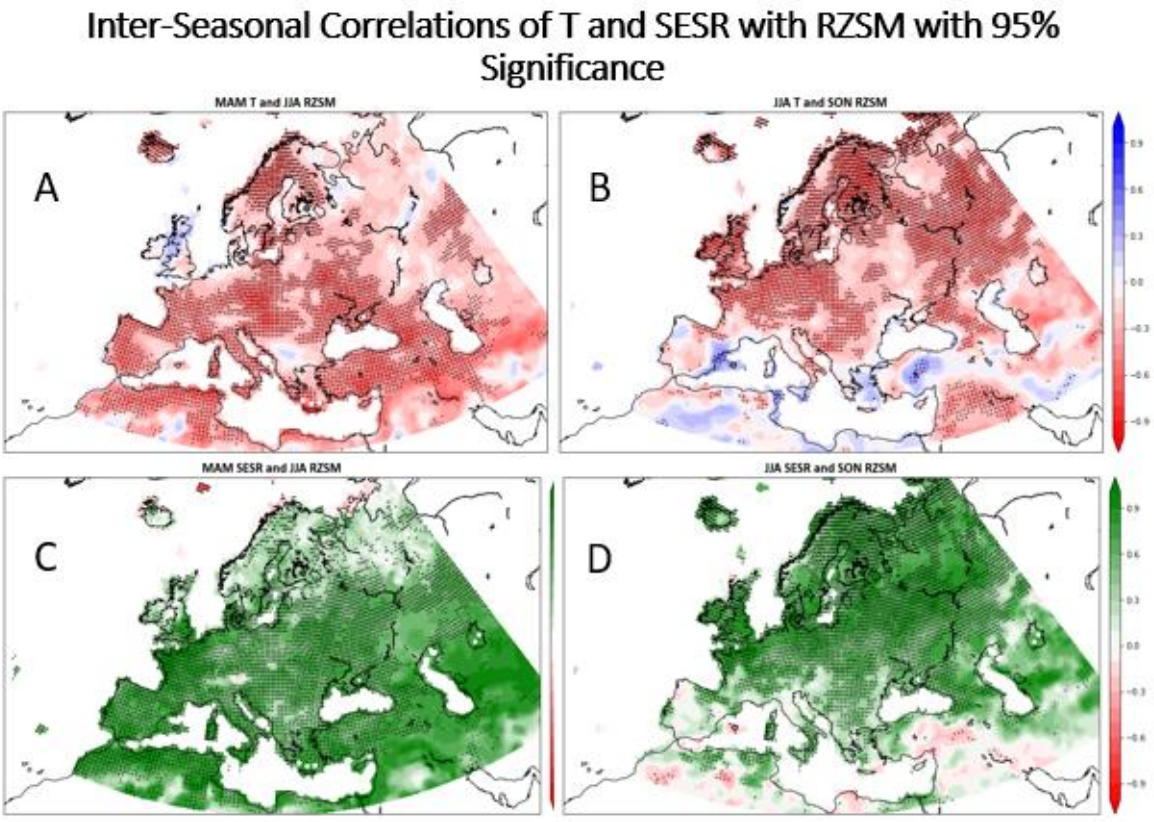

***Figure 2.2**. Inter-seasonal correlations for T and RZSM for a.) MAM to JJA respectively, and b.) JJA to SON. Correlations for SESR and RZSM for c.) MAM to JJA and d.) JJA to SON. All plots are overlaid with a stipple where grid points exceeded the 95% confidence threshold.*

Comparison of regions with a strong correlation between SESR and RZSM and those with negative correlations between T and RZSM can be used to identify areas that may be more prone to flash drought development. Although there is variation spatially between different seasons, much of Europe shows significant overlap between the lag regressions. This suggests that these areas are likely to experience reduced mean soil moisture levels based on the mean evaporative stress and temperature of the previous season.

2.3.3 Inter-seasonal multivariable regression

An inter-seasonal multivariable regression using RZSM as the predictand of T and SESR (Fig. 2.3a-d) shows that SESR is the stronger driver affecting RZSM during the following season. Over most of the continent, T does marginally influence seasonal RZSM, however there are several regions where evaporative stress plays a much larger role than T alone. These regions are largely consistent with the areas of higher correlation in Figures 2.2c and d. The comprehensive spatial extent of the strong lag correlations between SESR and RZSM implies that evaporative stress serves as a critical indicator of RZSM during the following season throughout most of the continent.

2.3.4 – Lag regressions compared to known past flash drought events

The introduction of lag into regression analysis has shown that regionally, the feedbacks between land and atmosphere can exist and persist on a seasonal to sub-seasonal timescale. Increased temperature leads to elevated ET which will begin to dry soils earlier in the year. If these higher temperature and ET levels continue, cascading effects can lead to flash drought. Figures 2.4, 2.5, and 2.6 are regional analyses of three major European flash drought events; France in 2003 (Fig. 2.4), Western Russia in 2010 (Fig. 2.5), and Belarus in 2015 (Fig. 2.6). All three events

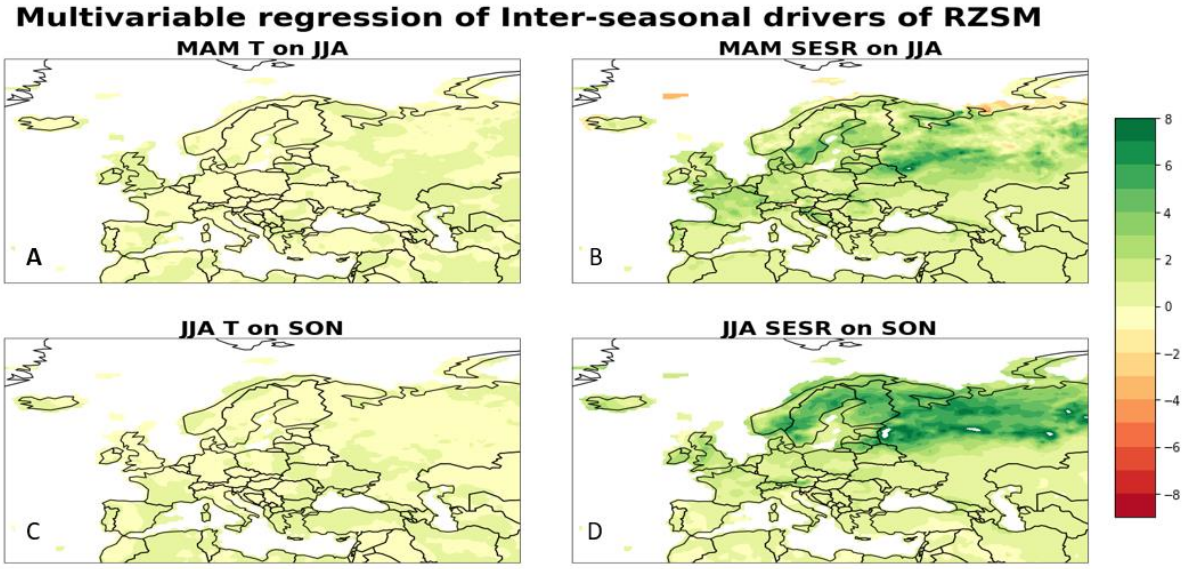

***Figure 2.3 (a-d)**. Inter-seasonal multivariable regression using T and SESR to predict RZSM. Values are the weight of each respective variable's contribution to the prediction of the following seasons RZSM.*

were preceded by areas of anomalously high spring mean temperatures, with some areas reaching close to 2 standard deviations above the mean. These seasonal T anomalies were accompanied by localized areas of increased evaporative stress. As the growing season progressed, the regions of higher temperatures/evaporative stress became areas of extreme evaporative stress. As such, these areas were identified as having negative SESR anomalies and were accompanied by large deficits in soil moisture, some as high as 5 to 7 standard deviations below the mean. Each of these flash drought events corresponds to areas in Figure 3a where MAM SESR is identified as a more predominate driver of JJA RZSM.

In each inset region two points were selected based on proximity to temperature anomalies. At each point a standardized time series of T, SESR, and RZSM was plotted

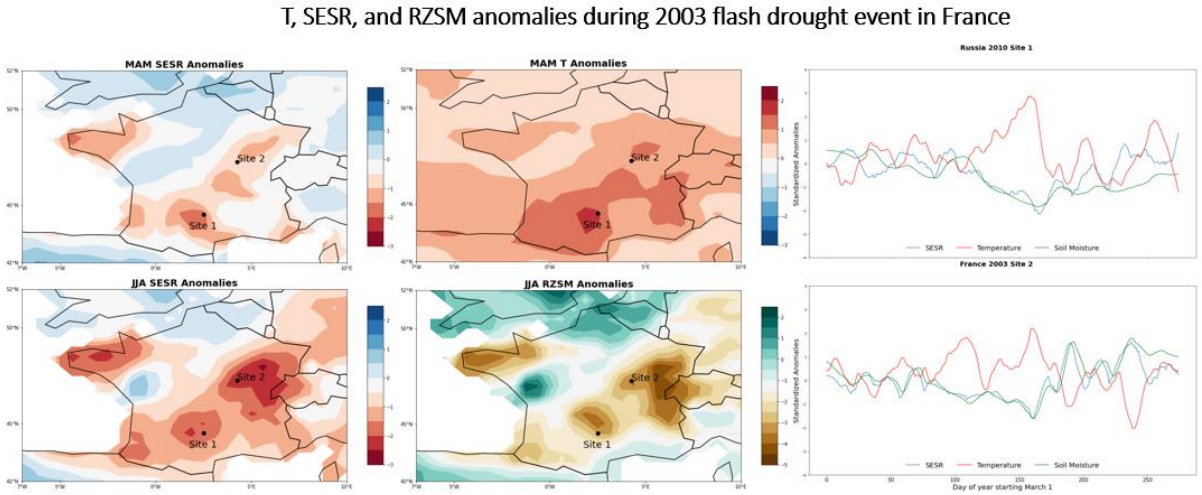

***Figure 2.4**. Anomalies from the 2003 flash drought in France. Included are plots of MAM SESR and T anomalies. These then progress to JJA SESR and RZSM anomalies. Timeseries from 2 grid points present the evolution of each variable beginning March 1 through the end of November.*

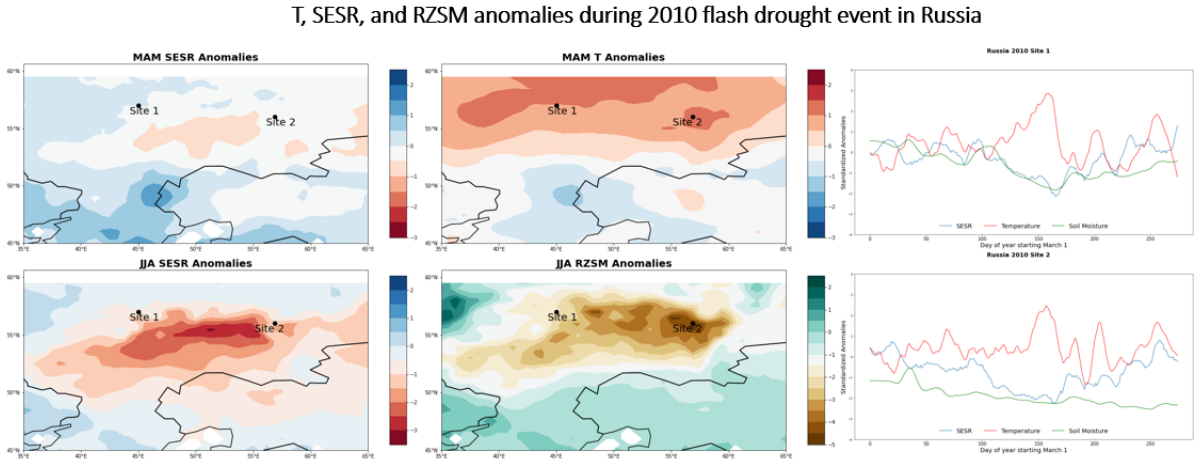

***Figure 2.5**. Anomalies from the 2010 flash drought in Russia. Included are plots of MAM SESR and T anomalies. These then progress to JJA SESR and RZSM anomalies. Timeseries from 2 grid points present the evolution of each variable beginning March 1 through the end of November.*

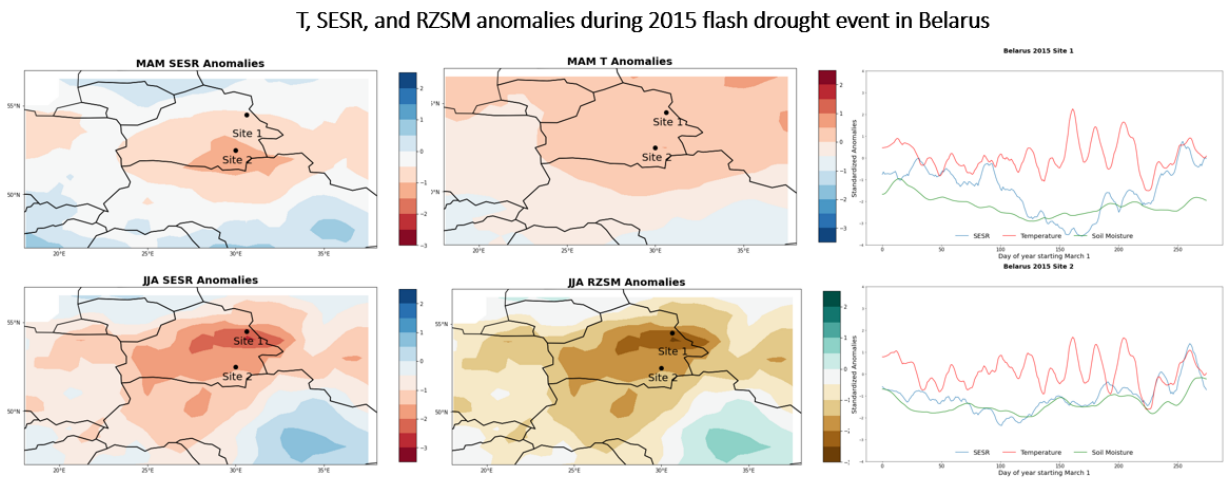

Figure 2.6*. Anomalies from the 2015 flash drought in Belarus. Included are plots of MAM SESR and T anomalies. These then progress to JJA SESR and RZSM anomalies. Timeseries from 2 grid points present the evolution of each variable beginning March 1 through the end of November.*

beginning March 1st, to track each variable's evolution throughout the spring and into the summer. The results show a period in the spring where standardized T begins to increase above the climactic norm. This is accompanied by a decrease in both SESR and RZSM. In all 6 timeseries, the vast difference between T, SESR and soil moisture becomes apparent during the flash drought events later in the growing season.

2.4 Discussion:

The results of this study demonstrate that, over a large spatial extent across Europe, a strong relationship exists between temperature, evaporative stress, and soil moisture, both concurrently and inter-seasonally. Because flash drought is largely driven by evaporative stress and its impact on soil moisture (Parker et al., 2021; Christian et al., 2019b; Otkin et al., 2019; Otkin et al., 2016; Ford et al., 2015), the strength and magnitude of seasonal evaporative stress

has utility to predict soil moisture desiccation and the possibility of agricultural flash drought development within a region.

Soil moisture is a key component of flash drought development (Seghal et al., 2021; Christian et al., 2020; Christian et al., 2019b; Otkin et al., 2016) but there can be large regional variations in soil properties and local climate. Here we have shown that despite the regional differences in soil types, SESR has a strong correlation with RZSM across most of Europe. As such, these results reinforce that evaporative stress and soil moisture are strongly coupled during the warm season across much of Europe. While temperature is the main regime that drives the fluctuations in evaporative demand in some regions (Azorin Molina et al., 2015; Hobbins et al., 2012), temperature alone may not be a good predictive metric for soil moisture. Conversely, while SESR is a function of temperature, it also accounts for many other near surface state variables, such as wind, vapor pressure deficit, and pressure. Regional variation will play a significant role in this process and there will be some lag from higher levels of demand to reduced RZSM levels due to soil moisture memory (Mukherjee et al., 2022a; Zhao et al., 2019; Miralles et al., 2012).

With the rise of global temperatures and the increased likelihood of future combined drought heatwave events (Mukherjee et al., 2022b; Rakovec et al., 2022; Hari et al., 2020; Samaniego et al., 2018; Bador et al., 2016b; Russo et al., 2014) an increased likelihood exists for periods of anomalously warm temperature earlier in the growing season. Hotspots created by uneven warming due to climate change are impacting Europe and notable, accelerated warming compared to the global average is occurring (Donat et al., 2017). As such, combined drought-heatwave events have increased agricultural loses and mortality rates when compared to either

event occurring on its own (Orth et al., 2022). Feedback loops where higher temperatures lead to increased ET and subsequent drier soils (Seneviratne et al., 2010) which yield further increases in mean temperature and the production of persistent heatwaves (Miralles et al. 2019) in the subsequent season. The 2003 European heat wave was an example of this process whereby early spring warmth led to soil moisture depletion early in the year (Fischer et al., 2007; Zaitchik et al., 2006) followed by record elevated temperatures and drought conditions for the remainder of the growing season.

Anomalously high, early-season temperatures can also lead to early green-up in vegetation which reinforces the feedbacks between T, evaporative stress and RZSM by increasing ET (Zaitchik et al., 2006; Fischer et al., 2007; Christian et al., 2019b; Christian et al., 2022). As such, an early green-up can be important during flash drought onset and set the stage for the rapid drying of soils within the growing season when flash drought occurrence is more likely (Christian et al., 2019b). Thus, an early reduction in RZSM can accelerate the evolution of flash drought from meteorological to agricultural drought as some vegetation, while under water stress, will not close stomata thereby increasing dehydration rates (Marchin et al., 2022; Buckley, 2019) yielding desiccation of both the soil and vegetation surfaces.

The strong correlation between T, SESR and RZSM for much of the central latitudes of Europe suggests that mean seasonal temperatures and evaporative stress could be used as a predictor for potential subsequent seasonal evaporative stress or soil moisture. Multiple regression has identified areas where seasonal SESR is a significant driver of growing season drying priming of these areas for cascading drought effects if conditions persist.

Flash drought is a critical extreme event that manifests as meteorological drought which rapidly accelerates the onset of agricultural drought. As the "nexus" between meteorological and agricultural drought, it can be difficult to find the best approach for forecasting flash drought onset. Precipitation is a critical metric defining meteorological drought however, soil moisture-based metrics better monitor agricultural drought (Chatterjee et al., 2022). The role of soil moisture is vital in agricultural drought due to its potential to influence critical and destructive impacts (Christian et al., 2021; Basara et al., 2019; Jin et al., 2019; Otkin et al., 2018a; Otkin et al., 2018b). A combined evaporative stress-soil moisture change indicator may offer the best overlapping metric to signal impending flash drought conditions (Anderson et al., 2013). Tools such as the Flash Drought Stress Index (Sehgal et al., 2021) that use the relative rate of drydown and offers a 0–2-week lead time has shown reliable results and may be enhanced using long term meteorological conditions. Further, the FLASH tool from National Ocean and Atmospheric Association's Climate Prediction Center has also shown good initial results (Chen et al., 2020); FLASH uses the Rapid Change Index (RCI; Otkin et al., 2014) to measure changes in ET along with deficits in the Standardized Precipitation Index to give 30-day outlooks for flash drought conditions. Adapting models like these with the addition of the inter-seasonal effects of early season T and SESR may offer increased forecast accuracy of flash drought onset.

2.5 Conclusions:

This study performed a regression analysis to identify the strength of relationships across Europe between temperature and evaporative stress with soil moisture during (a) concurrent seasons and (b) when a one-season lag was introduced. Using seasonal mean values,

Both T and SESR showed high correlations for much of the southern portion of the continent in all three concurrent seasons with those regions expanding during the summer. SESR and RZSM exhibited the strongest relationship with most of the continent above the 95% confidence level. Further, the introduction of the lag between T, evaporative demand, and soil moisture again had strong results showing their seasonal interaction can persist over longer temporal periods. Multivariable regression identified SESR as the predominant driver of subsequent seasonal RZSM levels. Many of the regions where RZSM was identified as more susceptible to increases in both T and evaporative stress correspond to areas where the largest European flash droughts occurred. The strong relationship between seasonal and inter-seasonal RZSM and SESR could bridge the gap between soil moisture and atmospheric based flash drought metrics and improve existing prediction models.

Chapter 3: Synoptic and Local Drivers of Regional Flash Drought in the United States

3.1 Introduction:

Flash drought is the rapid intensification of drought conditions (Otkin et al., 2018b; Christian et al., 2019b; 2021). While a meteorological phenomenon, flash drought can quickly progress into agricultural or hydrological drought that can be devastating to agricultural producers, natural ecosystems, and water supply security (Wilhite et al., 2007; Basara et al., 2013; Christian et al., 2019a, Wen et al., 2023, Christian et al., 2024). Flash droughts are a phenomenon that can occur in any season (Christian et al., 2019b; 2021) but most often occur in the warmer growing seasons.

There are many local factors that can influence flash drought development. For example, feedbacks between evaporative stress, temperature, and soil moisture have been shown to drive flash drought development (Otkin et al., 2014; Ford 2017; Christian et al., 2019a; 2021; Parker et al., 2021). Increases in evaporative stress drive increased evapotranspiration, which further leads to drying of the soils, decreased evaporative cooling, and increasing surface temperatures (Seneviratne et al., 2010). Consequently, increased surface temperatures increase evaporative stress. This cascading effect can very quickly lead to soil desiccation and vegetative stress or damage (Otkin et al., 2016; Tian et al., 2018; Christian et al., 2022;).

In the absence of precipitation, the cascading feedbacks can yield flash drought development in a matter of weeks (Basara et al., 2019; Christian et al., 2020). Flash droughts can

appear quickly from what would be considered neutral or even wet conditions (Hoerling et al., 2014; Otkin et al., 2018b; Bolles et al., 2021; Osman et al., 2022;) catching managers and planners unprepared. Understanding the preceding conditions that drive the cascade to flash drought is critical in being better prepared for such whiplash conditions.

There are multiple drought and flash drought indices and prediction models such as the Standardized Evaporative Stress Ratio (SESR; Christian et al., 2019b; 2021), the Rapid Change Index (RCI; Otkin et al., 2014), the Palmer Drought Severity Index (PSDI; Palmer 1965), the Flash Drought Tool (Chen et al., 2020), and statistical models added to the Climate Forecasting System (Lorenz et al., 2018). These indices are primarily based on changes in variables such as evaporation, soil moisture, or precipitation. While there has been success in monitoring and detection of flash drought using these methods, questions remain regarding the larger atmospheric circulation patterns and processes that drive flash drought onset and development.

Atmospheric ridging has been shown to be an important feature of flash drought development (PaiMazdur & Done, 2016; Ford & Labosier 2017; Basara et al., 2019; Bolles et al., 2021; Jong et al., 2022; Kautz et al., 2022) though what mechanisms that cause ridges to form during flash drought periods is poorly understood. Atmospheric ridging can be the result of internal variability (Seager et al., 2016), but can also be related to sea surface temperature variability (SST). Recent work has shown that North Pacific ridging over the West Coast of North America can be caused by remote teleconnections via tropical excitation of Rossby waves (Seager & Henderson, 2015; Swain et al., 2017). It is well documented that SST variation plays a strong role in North American precipitation patterns, most notably through the El Niño-Southern Oscillation (ENSO; Rasmusson & Carpenter, 1982; Flanagan et al., 2018; 2019). Changes in the

mode of ENSO are known to bring drought conditions to many regions of the globe (Singh et al., 2021; 2022) including parts of North America.

Teleconnections with remote SSTs may be a driving force of the atmospheric ridging that is often associated with flash drought development. As such, this study will examine flash drought development by (1) identifying synoptic scale drivers that may be caused by teleconnections from changes or oscillations in SSTs, (2) how these changes can impact larger atmospheric circulation patterns, and (3) how the changes in larger circulation patterns interact at a local scale to drive flash drought conditions.

3.2 Methodology:

Because agriculture is particularly susceptible to flash drought, two study areas were selected to examine the larger atmospheric and regional drivers of flash droughts in the United States. The first area spans the Southern Great Plains (SGP) and is represented by the coordinates 32-38°N Latitude and 93.5-102°W Longitude which roughly comprises the state of Oklahoma and portions of the surrounding states. The second area is bounded 40 - 45°N and 89.5 - 99°W and includes Iowa and portions of the surrounding states in the Midwest (MW). Both areas are prone to and contain ecosystems susceptible to flash drought development (Christian et al., 2020; Fellman et al., 2023).

Individual flash drought events were identified via the Standardized Evaporative Stress Ratio (SESR) using data collected from the ERA5 reanalysis. SESR was calculated via Christian et al. (2019a; 2021), where the Evaporative Stress Ratio (ESR) is standardized to provide a more robust metric for analysis of atmospheric evaporative stress. ESR is the ratio of

Evapotranspiration (ET) to Potential Evapotranspiration (PET) and is standardized by removing the mean and dividing by the standard deviation. Rapid declines in SESR, in periods as short as 4-5 weeks, indicate increasing evaporative stress critical to identify flash drought development (Christian et al., 2019a; 2019b; 2021; Edris et al., 2023; Nguyen & Choi, 2024).

The most damaging flash droughts occur during the growing season (April – September) and can occur multiple times within a region during a single year whereby subsequent events can be impacted by the environmental memory of previous flash drought occurrence (Christian et al., 2024). As such, to focus on the teleconnections and drivers that lead to independent flash drought development, the earliest growing season events were selected to avoid impact of landscape memory from previous events. Flash droughts are commonly studied during the summer months (June, July, and August). With spring phenology occurring earlier in the year (Cong et al., 2013), and the occurrence of notable flash droughts occurring early in the growing season (Christian et al., 2021), April 1st was identified as the threshold for the earliest event considered in this study.

To isolate single events that occurred in the same temporal span (Fig. 3.1), a threshold of 30 days was used to identify the datapoints for each flash drought event in the selected study area. Any datapoint that registered a flash drought start date within 30 days of the first datapoint in that respective study area, were considered a single event. All other datapoints were excluded to eliminate secondary events or events that occurred independent of the selected event but did not overlap. In addition, the total number of datapoints identified in that 30-day window needed to exceed 175, or approximately 20% of the respective study area.

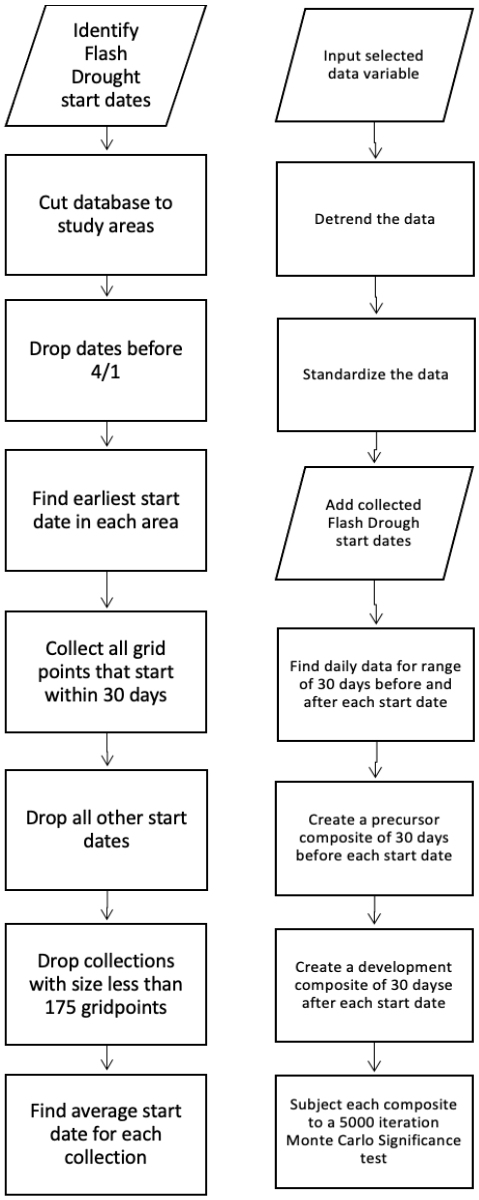

Figure 3.1*. Flowchart showing the process of selecting flash drought years and the creation of both antecedent and development composites.*

Table 3.1. *Flash drought years selected for each location using the methodology outlined in figure 1.*

Southern Great Plains	Midwest
1980, 1984, 1988, 1990, 1994, 2000, 2004, 2006, 2009, 2011, 2012, 2017	1988, 1989, 1991, 1992, 2006, 2009, 2012, 2017

To create a composite of precursor flash drought conditions, only events in these two months were selected. The resultant years (Table 3.1) are congruent with what would be expected when only early-season flash droughts are selected. In the Southern Great Plains flash droughts are expected 1 out of every 3 years (Lesinger & Tian, 2022; Christian et al., 2019b) and represent approximately 28% of years in the data set. In the Mid-west study region, fewer events were identified but still represented approximately 18% of years.

To calculate a start date for each event, the mean date was calculated for all datapoints that registered during each respective year's event. Using this selection of start dates, all variables were amassed in 2 collections. The "Antecedent" collection is 30 days before the start date in each respective year while the "Development" collection is the start date to 30 days after. Next, these 30-day windows from all years within each respective collection were used to create composite analyses. Thus, the precursor composites represent the 30 days leading up to the initial decline in SESR values. The development composite follows the first 30 days through the decline of SESR and corresponds to the "flash" period of flash drought.

Data 3.2.1:

Comprehensive analysis of teleconnections affecting CONUS requires large spatiotemporal datasets. Atmospheric reanalysis data collected from the European Center for Medium-Range Weather Forecasts version 5 (ERA5) provides hourly estimates from 1940 to the present. Data from 1980 through 2022 was collected at a resolution of 0.25° which was coarsened to 0.5° to accommodate the large spatial area of analysis.

A known, critical driver of precipitation patterns within CONUS is the Pacific El-Nino Southern Oscillation (Rasmusson & Carpenter, 1982; Flanagan et al., 2018; 2019) and semi-regular changes in Pacific Sea Surface Temperature (SST) impact water vapor transport (Flanagan et al., 2017; 2018). To examine both ENSO and the North Atlantic Oscillation and their effect on flash drought development, a scale of 30°S to 90°N Latitude and 0°E to 180°W was used to represent composite patterns across both oceans along with the CONUS region and patterns of Geopotential Heights along with U and V winds were analyzed.

While precipitation is influenced by synoptic ocean and atmospheric conditions but it's spatial occurrence over land directly impacts flash drought development. Soil Moisture (SM), SESR, and vegetation density can have interlocked effects on both atmospheric and terrestrial conditions in a region (Ma et al., 2019; Li et al., 2021; 2022). Areas bound by the SGP and MW study areas were used to examine these local land-atmosphere effects at regional scales to identify their roles in regional flash drought development. The Enhanced Vegetation Index (EVI) is a measure of canopy density. EVI is a modified version of the Normalized Difference Vegetation Index (NDVI) with an adjustment for soil and aerosol scattering in the blue bands. EVI has been shown more effective in areas of high biomass than the NDVI (Jensen, 2007). Finally, 2-meter temperature (T) is an atmospheric variable largely influenced by land surface conditions. As such, T conditions were examined on a continental scale to better connect influence of atmospheric patterns on T synoptically and locally. After mean composites were calculated, significance was tested using a bootstrapping simulation. N = 10,000 resamples were conducted and the distribution compared to alpha values of ± 0.05.

3.3 Results:

3.3.1 Synoptic drivers of flash drought in the SGP

Synoptic scale atmospheric ridging is often linked to SSTs. As such, to understand flash drought development SST and atmospheric conditions were examined. Figure 3.2a displays the 30-day composite of antecedent SST conditions prior to flash drought onset in the SGP. Overall Pacific SST anomalies display cooling in the Central and Eastern Pacific consistent with a La Niña pattern of ENSO. Further, the atmospheric conditions yield a negative 500 mb anomaly that extends over much of the Pacific and into the Atlantic with negative U wind anomalies at 250 mb (Fig. 3.2b) consistent with a southern shift in the subtropical jet.

Additionally, an area of increased anomalous temperature appears in the North-central Pacific that registers as statistically significant (Fig. 3.2a). This area is coupled with cooler SST temperatures to the north that are accompanied by a significant minimum in GPH. A geopotential high anomaly is co-located with the high SST anomalies and extends to the US West Coast. Wind anomalies include positive U wind anomalies adjacent to the Pacific Northwest along with anomalous V winds further northward (Fig. 3.2c). The wind patterns reflect the cyclonic flow in the North Pacific low and a dip in the polar jet over the Pacific that then moves back north as it approaches North America.

Divergence of the polar jet and weakened pacific jet is associated with La Nina pattern ENSO (Becker, 2023). The low geopotential heights at both 500 and 250 mb centered over the cooler SSTs are a critical significant synoptic feature. Combined with an area of anomalously high 500 mb values that extends in a flat pattern from the North Central Pacific (NCP) over

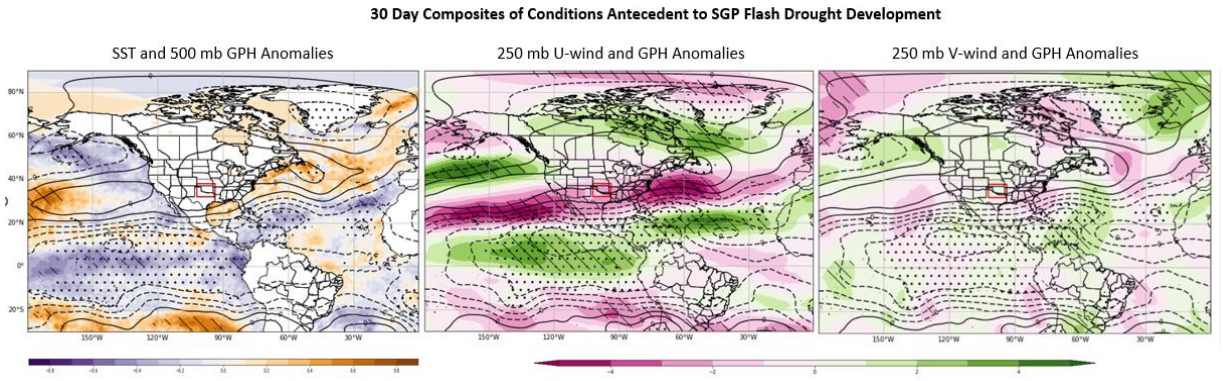

Figure 3.2 (a-c). *Mean composite of conditions 30 days prior to flash drought onset for dates and years in the Southern Great Plains. a. Sea Surface Temperature and 500 mb geopotential height standardized anomalies. b. 250 mb U-wind anomalies in m/s and c. 250 mb V-wind anomalies in m/s. Stippled areas indicate statistically significant GPH anomalies and diagonal lines represent significant SST and wind anomalies in each respective plot.*

North America and into the Northeast and Central Atlantic (Fig. 3.2a) the overall, the Rossby wave pattern represented by these anomalies yield a very low amplitude. The low amplitude Rossby wave train forces the subtropical jet to pass south of CONUS. Conversely, anomalous easterly winds (i.e., weaker westerlies) occur north of the subtropical jet over the southern US yielding a weaker storm track.

Downstream of the study area, significant, anomalously high values of geopotential height in the Northwest Atlantic and adjacent regions of North America are co-located with anomalously warm SSTs in the North Atlantic. The SST anomalies in the North Atlantic combined with the northward displacement of the U-wind anomalies resemble a positive phase of the North Atlantic Oscillation (NAO; Cassou, 2008).

3.3.2 Local Drivers in the SGP

Precipitation is the first order driver of drought, however in the SGP increased precipitation is a significant antecedent condition prior to flash drought (Fig. 3.3b). This area is known for mesoscale convective events during the spring season (Reif & Bluestein, 2017). These more localized events may account for the positive precipitation anomalies despite the larger synoptic patterns being unfavorable for consistent precipitation occurrence. The enhanced localized precipitation is also likely responsible for the positive soil moisture anomalies present during flash drought years (Fig. 3.3c). While the higher soil moisture anomalies do not perfectly co-locate with the precipitation anomalies, overlapping areas of significance do occur.

Antecedent surface temperature seems to play a minimal, consistent role in flash drought development in the SGP. While the standardized anomalies are positive throughout the study area, they are nearly zero for most of the domain. The composite results also show minimal significance except for a small area in the southeast near areas of greater temperature anomalies. Anomalously high moisture likely reduces surface temperature through diabatic cooling (Seneviratne et al., 2010).

Despite increased moisture, vegetation densities show inconsistent anomalies. Areas co-located with increases in soil moisture show minimal or decreased EVI anomalies. Ecosystem response to increased moisture combined with normal temperatures in these areas may not support early year growth anomalies.

3.3.3 Flash drought development in the SGP

The 30-day period beginning with the decline of SESR into flash drought conditions is defined as the development phase. Synoptically, during the development phase a synoptic pattern

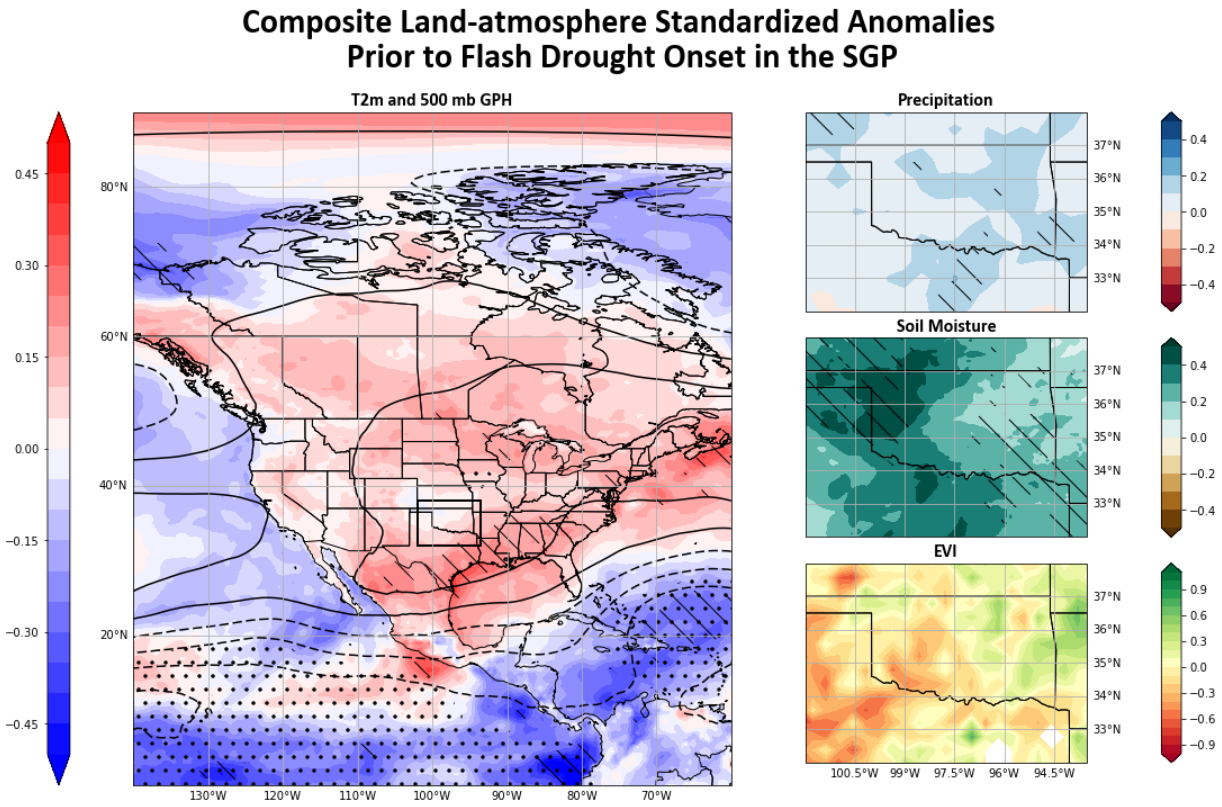

Figure 3.3 (a-d). *Mean composites of 30 days antecedent to date and year of flash drought onset in the Southern Great Plains. a. 2-m temperature standardized anomalies. Dashed overlays indicate statistical significance above 90% for temperature, and stipples indicate significance for e500 mb GPH., b. precipitation standardized anomalies, c. soil moisture standardized anomalies, and d. Enhanced Vegetation Index anomalies. Dashed lines for b-c indicate significance above 90%.*

shift was noted. First, while the composite values are less intense, SST anomalies are similar and change little when compared to the antecedent period (Fig. 3.4a). This result is not surprising given the longer temporal span required for changes in SST to occur.

The most prominent 500 mb GPH feature of the composites for the development period is the large trough located off the West Coast of the US. The trough (Fig. 3.4b) is part of a Rossby wave train that has an increased amplitude compared with the antecedent period (Fig. 3.2b). In addition, a pronounced atmospheric ridge is centered over the SGP and Northern Mexico. This positioning of the ridge is significant and would account for conditions that would favor flash drought to occur including large scale subsidence, reduced precipitation, and increased solar insolation.

The absence of strong u-wind anomalies suggests a retrograde of the zonal winds implying stationary atmospheric conditions, and as such, a blocking ridge across the SGP along with elevated temperature anomalies centered under the ridge.

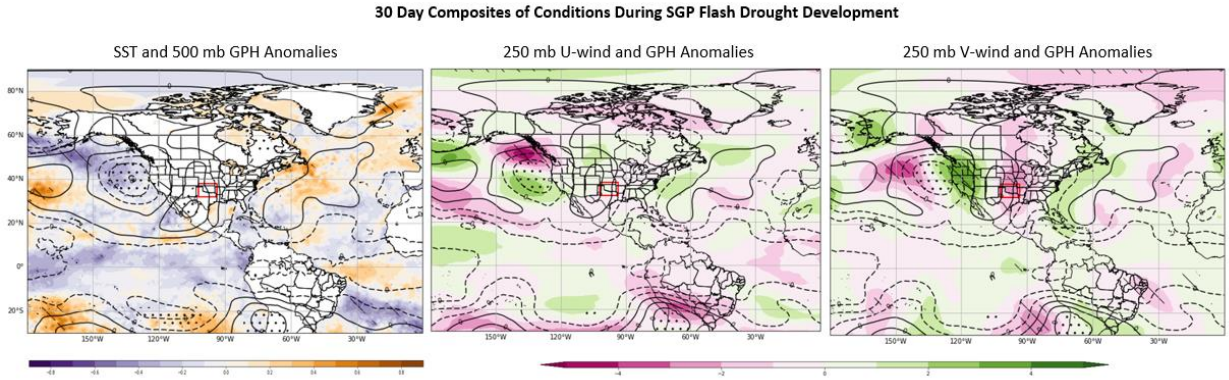

Figure 3.4 (a-c). Mean composite of conditions 30-days during flash drought development for dates and years in the Southern Great Plains. a. Sea Surface Temperature and 500 mb geopotential height standardized anomalies. b. 250 mb U-wind anomalies in m/s and c. 250 mb V-wind anomalies in m/s. Stippled areas indicate statistically significant GPH anomalies and diagonal lines represent significant SST and wind anomalies in each respective plot.

While composite values of soil moisture tend to be above normal during the period within the domain (Fig. 3.5c), the values are less than the antecedent period reflective of overall drying during the temporal window. Further, negative vegetation impacts are apparent during this phase (Fig. 3.5d).

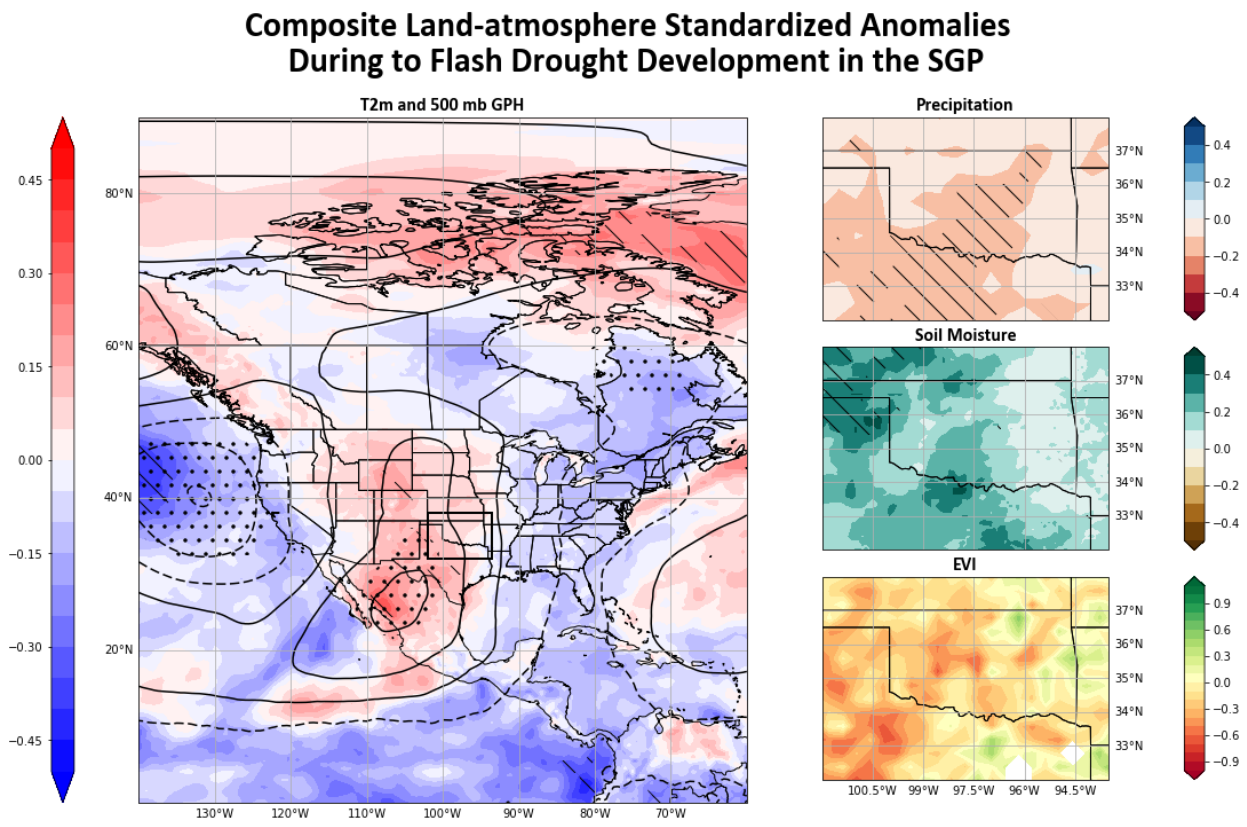

Figure 3.5 (a-d). *Mean composites of 30 days after date and year of flash drought onset in the Southern Great Plains. a. 2-m temperature standardized anomalies. Dashed overlays indicate statistical significance above 90% for temperature, and stipples indicate significance for e500 mb GPH., b. precipitation standardized anomalies, c. soil moisture standardized anomalies, and d. Enhanced Vegetation Index anomalies. Dashed lines for b-c indicate significance above 90%.*

3.3.4 Synoptic drivers of flash drought in the MW

Composite of antecedent synoptic conditions for MW flash droughts display a well-defined Omega block wave pattern (Figs. 5a-c; Rex, 1950). As such, the areas of increased GPH anomalies consistently occurred during the antecedent period before flash drought onset in the MW domain, two of which are centered over areas of anomalously warm SSTs in both the North-central Pacific and Atlantic. In between, a pronounced, and statistically significant ridge is centered across North America from Northern Mexico to the Arctic. As a result, zonal winds

(Fig. 3.5b) across the CONUS are dramatically reduced with a split-flow patten yielding enhanced westerlies in the arctic and Central America. Further, the meridional winds resemble the Omega block pattern (Fig. 3.5c).

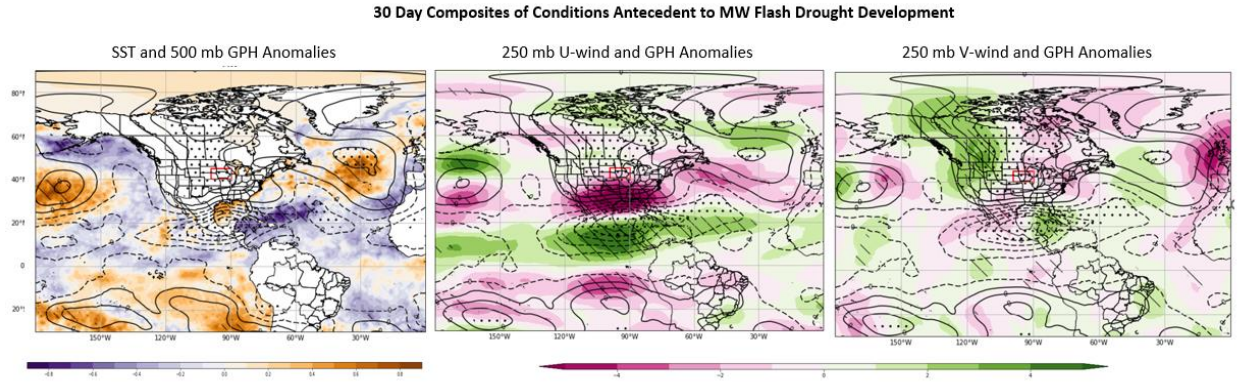

Figure 3.5 (a-c). *Mean composite of conditions 30-days prior to flash drought onset for dates and years in the Midwest location. a. Sea Surface Temperature and 500 mb geopotential height standardized anomalies. b. 250 mb U-wind anomalies in m/s and c. 250 mb V-wind anomalies in m/s. Stippled areas indicate statistically significant GPH anomalies and diagonal lines represent significant SST and wind anomalies in each respective plot.*

3.3.5 Local Drivers in the MW

The 30-day composite of 2-m temperature for MW flash droughts yields significant warming for much of North America. The greatest temperature anomalies are located in the Central US, with significant anomalies located to the south of the MW flash drought domain (Fig. 3.6a).

Precipitation and moisture anomalies during the antecedent period for the MW are near the composite mean while EVI is elevated associated with enhanced vegetation conditions. The elevated EVI is an indicator of enhanced greenup and is likely due to increased temperature along with sufficient soil moisture.

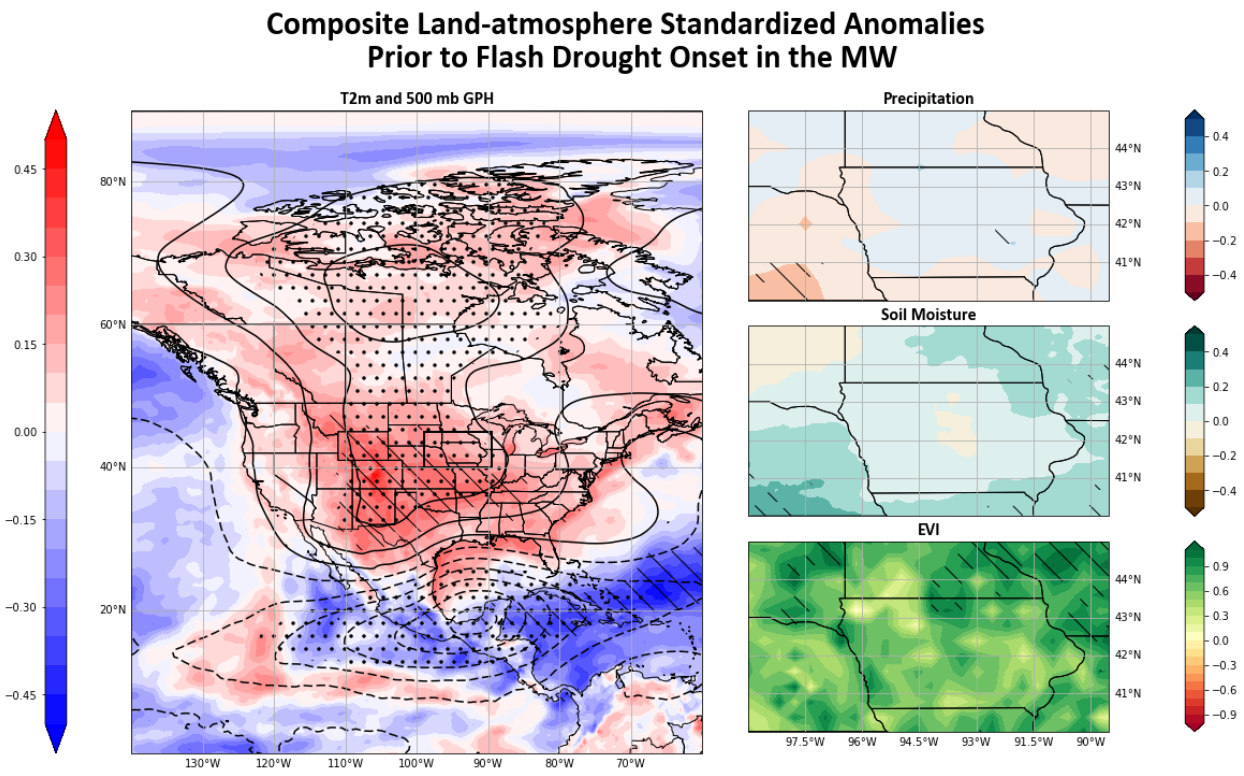

Figure 3.6 (a-d). *Mean composites of 30 days prior to date and year of flash drought onset in the Midwest location. a. 2-m temperature standardized anomalies. Dashed overlays indicate statistical significance above 90% for temperature, and stipples indicate significance for e500 mb GPH., b. precipitation standardized anomalies, c. soil moisture standardized anomalies, and d. Enhanced Vegetation Index anomalies. Dashed lines for b-c indicate significance above 90%.*

3.3.6 Flash Drought Development in the Midwest

Composites for the development phase within the MW domain display a different overall synoptic pattern compared with the antecedent period. (Fig. 3.7) Thus, during the development phase, a more defined Rossby wave train is present with alternating troughs and ridges extending east-west within the mid latitudes and an overall composite ridge axis to the west of the MW domain with a trough to the east.

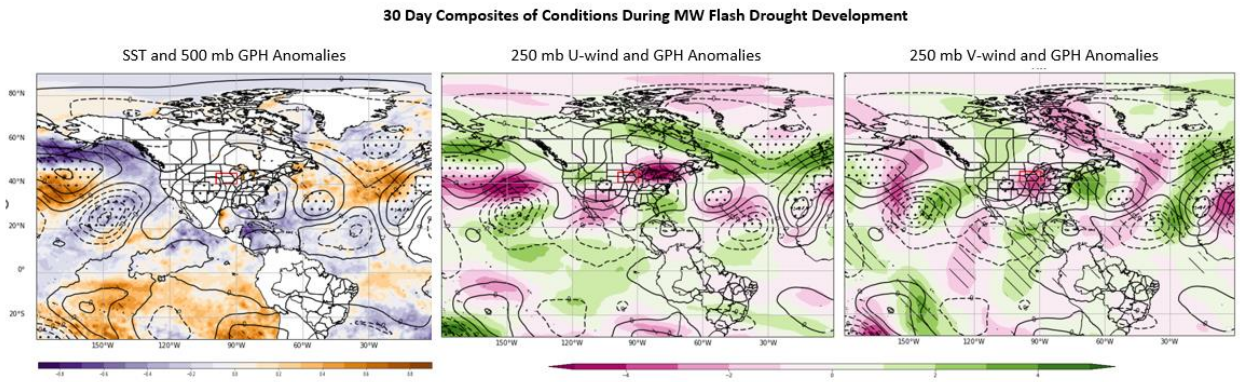

Figure 3.7 (a-c). *Mean composite of conditions 30 days after to flash drought onset for dates and years in the Southern Great Plains. a. Sea Surface Temperature and 500 mb geopotential height standardized anomalies. b. 250 mb U-wind anomalies in m/s and c. 250 mb V-wind anomalies in m/s. Stippled areas indicate statistically significant GPH anomalies and diagonal lines represent significant SST and wind anomalies in each respective plot.*

Further, due to the orientation of the ridge to the west and a trough to the east, the overall westerlies across the domain are reduced compared to the mean conditions (Fig. 3.7b), with a strong northerly component of the meridional wind directly overhead of the domain (Fig. 3.7c).

At the surface, warm temperature anomalies are generally co-located with increased 500 mb GPH anomalies during the development phase with an area of statistically significant values centered just to the southwest of the study area. The study area is also represented by statistically significant precipitation deficits along with decreases in both soil moisture and EVI. In addition, the decline of EVI is quite dramatic but expected during agricultural droughts Christian et al., 2020;2022;2024; Fellman et al., 2023).

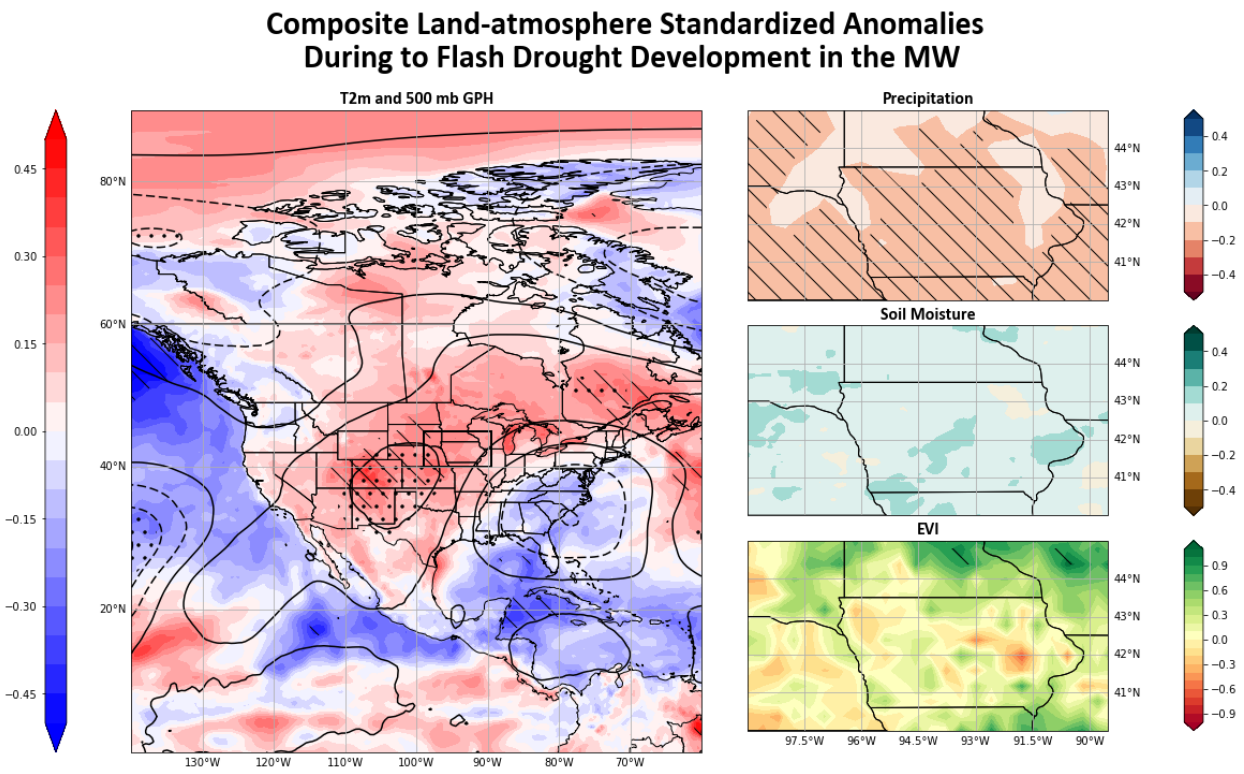

Figure 3.8 (a-d). *Mean composites of 30 days after to date and year of flash drought onset in the Midwest location. a. 2-m temperature standardized anomalies. Dashed overlays indicate statistical significance above 90% for temperature, and stipples indicate significance for e500 mb GPH., b. precipitation standardized anomalies, c. soil moisture standardized anomalies, and d. Enhanced Vegetation Index anomalies. Dashed lines for b-c indicate significance above 90%.*

3.4 Discussion:

This study created mean anomaly composites of synoptic scale processes prior to and during flash drought development. Antecedent condition composites for both the SGP and MW showed significant sea surface temperature anomalies in both the Atlantic and Pacific. For example, composite analyses for SGP flash drought events display a combined signal of weak La Nina phase ENSO and positive North Atlantic SSTs. Lesinger & Tian (2022) found that during La Nina phase and positive NAO, severe soil moisture deficit flash droughts increased from ~5% to ~15% and an increase of ~4% with positive NAO. The composites for this study represent

flash droughts driven by evaporative stress. While surface moisture deficits are part of evaporative stress, differentiation of distinct types of flash droughts are not directly accounted for, the results of this study are in agreement with Lesinger & Tian, (2022) whereby teleconnections with both Pacific and Atlantic variability exist and can lead to flash drought events in the SGP.

Shifts in the Pacific jet can alter the wave train patterns over the SGP and are known to affect moisture flow in the boundary layer (Flanagan et al., 2018). This study noted that enhanced zonal winds are present prior to flash drought development in the SGP with specific anomalies present both north and south of the study region representing a split flow pattern, weak ridging, and a limited storm track across the SGP region.

Antecedent conditions for MW flash droughts are quite different than those of the SGP. While the SGP is dominated by La Nina pattern SSTs, a significant area of warm SST anomalies occurs in the North Central Pacific and North Central Atlantic. The influence of Atlantic SST anomalies and corresponding GPH anomalies look to play a significant role in flash drought formation in the Central United States. Because changes in SST are slow to manifest, these could influence long term ridging that would slow the Rossby wave train. These warm anomalies form a large amplitude omega blocking pattern that occurs over North America. Droughts in the Central US are often linked to subsidence caused by persistent ridging (Cook et al., 2022; Jong et al., 2022; Basara et al., 2019) and both the SST and synoptic patterns are consistent with previous studies that show upstream synoptic features create the amplified atmospheric ridging that drives flash drought development (Ford and Labossier, 2017; Jong et al., 2022).

While regions can react differently to flash drought occurrence both areas of interest showed similar antecedent trends with pronounced ridging prior to flash drought development. At the same time, composite antecedent precipitation anomalies in the SGP display anomalously high conditions. While not the same in the MW areas of higher precipitation registered as statistically significant within the study domain. These findings are consistent with others that flash droughts often appear without warning (Osman et al., 2022; Bolles et al., 2021; Otkin et al., 2018b; Hoerling et al., 2014).

Increases in spring precipitation and warmer temperatures can contribute to increased spring vegetation densities and earlier spring phenology (Cong et al., 2013). These conditions would be consistent with what has been termed “early green-up” where vegetation response to conditions is to grow faster and mature earlier in the season (Stefanon et al., 2012; Cong et al., 2013). EVI anomaly composites show increased vegetation density prior to FD onset and regions of the MW exhibit anomalous vegetation growth prior to FD that is statistically significant. This is consistent with other previous case studies whereby large FD events can be preceded by an early green-up (Zaitchik et al., 2006; Fischer et al., 2007; Christian 2019b; 2022) that can contribute to quicker soil desiccation upon changes in evaporative demand.

The large area of North Pacific SST anomalies during MW drought years (Fig. 3.7a) is consistent with the area of Rossby wave packet origination that occurs during previously recognized Ohio Valley flash drought years (Jong et al., 2022). This area is significant during antecedent conditions in both composites. Downstream propagation of these wave packets helps to reinforce the stationary ridges that develop to the west of each study region. Anomalous stationary ridges induce strong downstream subsidence and result in low-level divergent outflow

(Jong et al., 2022). Subsidence induced drying influences the local land-atmosphere interactions that lead to depletions of soil moisture and drive higher surface temperatures.

Because flash drought can be devastating to agriculture and in situ ecosystems it is often viewed from the perspective of agricultural drought (Bajgain et al., 2017; Christian et al., 2022; Edris et al., 2023; Fellman et al., 2023). Tracking changes in intensity and propagation of agricultural flash drought often reveals stark depletions of soil moisture and vegetation health (Christian et al. 2020; 2024; Fellman et al., 2023). Changes between soil moisture and EVI anomalies between antecedent and development figures (Figs. 3.3 and 3.5; 3.6 and 3.8) are mean values for each period and do not represent the total changes from beginning of event to end of event. As such, they offer a change in mean values and not a change in absolute values.

Currently flash drought prediction is challenging (Otkin et al., 2022). Understanding the complex relationship between synoptic scale and local variability is necessary to better create prediction models (Pendergrass et al., 2020). The analyses shown here between remote SSTs, their connections with larger atmospheric mechanisms, and their influence regionally define patterns that provide a base for testing against current or future flash drought predictive models.

3.5 Conclusion:

To predict flash drought, we need to better understand the physical processes that drive flash drought development (Pendergrass et al., 2020). Many flash drought studies are from an agricultural perspective and focus on regional and local drivers and impacts. Land-atmosphere interactions are extremely important to flash drought development, however larger scale synoptic atmospheric processes drive the local scale ones. Fewer studies focus on these processes. In

terms of seasonal or subseasonal prediction of flash drought these synoptic scale processes become more important.

This study analyzed synoptic scale patterns that lead to flash drought in multiple regions in the US. SST anomalies in both the upstream Pacific and the downstream Atlantic play a role in flash drought formation. Antecedent condition composites demonstrated that Flash Drought occurrence can be directly related to SST conditions in both the Pacific and Atlantic. Strong positive anomalies are present in the North-Central Pacific in both the SGP and MW composites. The SGP composite also shows a weak negative ENSO pattern with associated GPH and wind anomalies. The MW composite shows strong omega pattern blocking with significant highs over North America. Despite increased temperatures, regional antecedent conditions exhibit little hint that flash drought is eminent with high precipitation and soil moisture anomalies.

Transitioning to flash drought development phase composites show changes in Rossby wave amplitude and frequency. Weaker zonal wind anomalies are present in both composites suggesting slower Rossby wave packet movement. The development of stationary atmospheric ridges over and adjacent to the study regions drive subsidence that yields local drying and increases in temperature. Locally, as expected, subsidence and decreased precipitation occur soil moisture and vegetation densities decrease as flash drought impacts grow in intensity.

Chapter 4: Examination of Synoptic Scale Remote Drivers of Evaporative Stress in the Central United States

4.1 Introduction:

Rapid declines in soil moisture are the result of feedbacks between land and atmosphere driven by evaporative stress (Otkin et al., 2014; Ford & Labosier, 2017; Christian et al., 2019b; 2021; Parker et al., 2021). Increases in evaporative stress and demand in the Central US have been shown to be the result of atmospheric ridging (Ford & Labosier, 2017; Basara et al., 2019; Cook et al., 2022; Jong et al., 2022; Chapter 3). Atmospheric ridges represent areas of increased atmospheric temperature and pressure due to subsidence. During flash drought development these ridges have been observed west of regions that develop flash drought (Ford & Labosier, Jong et al., 2022; Chapter 3) and inhibit moisture transport needed for precipitation.

Flash drought is complex and driven by synoptic scale processes in combination with local land-atmosphere interactions (Christian et al., 2019b; 2021, Jong et al., 2022). This combination of local and remote drivers makes flash drought challenging to predict (Pendergrass et al., 2020; Otkin et al., 2022; Chapter 3). Composites of Sea Surface Temperature (SST) standardized anomalies show areas that influence flash drought development in different regions of the Central US (Chapter 3). Above normal SST in the North Central Pacific (NCP) is associated with formation of high-pressure anomalies during flash drought years (Chapter 3). Rossby wave packets of high-pressure developed in the NCP have been shown to create atmospheric ridging that will stall over the Ohio Valley of the Central US during flash drought years. (Jong et al., 2022; Chapter 3). Flash droughts in the Southern Great Plains (SGP) are

associated with positive NCP anomalies (Chapter 3) along with weak La Nina phase El Nino Southern Oscillation (ENSO) in the Pacific and positive North Atlantic Oscillation (NAO; Lesinger and Tian, 2022; Chapter 3).

Changes in SST drive atmospheric pressure anomalies that influence Rossby wave amplitudes and frequencies. Changes in the wave properties alter wind direction and influence moisture transport from the tropics (Jong et al., 2022; Chapter 3). Moisture deficits are the primary driver of drought. Precipitation deficits combined with subsidence from stalled atmospheric ridges create the evaporative demand that cause rapid soil desiccation and agricultural flash drought (Otkin et al., 2014; 2018; Basara et al., 2019; Christian et al., 2019b; 2021; 2024; Jong et al., 2022, Chapter 2; 3).

To better predict flash drought the lag time between remote anomalous ocean and atmospheric process and subsidence that causes flash drought needs to be better understood and quantified. Early Spring jet motion has shown to move Rossby wave packets from the NCP through to the Atlantic in as little as 5 days (Jong et al., 2022), however this rapid motion and the Rossby packets slow over the course of the season with retrograde and narrowing of the jet (Newman & Sardeshmukh, 1998; Jong et al., 2022; Chapter 3).

Building upon the composites that were created in Chapter 3, this study will calculate the statistical validity of the recognized SST and 500 mb GPH patterns that led to flash drought development in the Midwest (MW) and Southern Great Plains (SGP) of the Central US. EOF modes and PC time series will be calculated and the spatial representations of the first 3 EOF modes will be compared with the corresponding composites from chapter 3. Temporal lag will be introduced to examine the variability between the remote drivers and local evaporative stress.

The PC time series will then be compared with changes in evaporative stress during different lag periods to assess the statistical correlations between large atmospheric patterns and local impacts.

4.2 Methods:

Atmospheric reanalysis data from the European Center for Medium-Range Weather Forecasts version 5 (ERA5) was collected and utilized for SST, 500 mb GPH, evapotranspiration (ET), 2-m wind speed (U_2), net solar radiation at the crop surface (R_n), temperature (T), soil heat flux density (G), saturation vapor pressure deficit (e_s), vapor pressure (e_a), the slope vapor pressure curve (Δ), and the psychrometric constant (γ) from January 1, 1980, through December 31, 2023. U_2, R_n, G, T, e_s, e_a, Δ, and γ were used to calculate potential evapotranspiration (PET) via the FAO Penman-Monteith equation (eq. 2.1; Allen et al., 1998). PET is a representation of the amount of ET that would occur with sufficient moisture to match demand within the system. The ratio of ET to PET is referred to as the Evaporative Stress Ratio and is a metric of evaporative demand (Otkin et al., 2018a; Christian et al., 2019). Following the method in Christian et al., (2019; 2021; eq. 2.2), standardization of the ESR was performed to create a more robust metric of evaporative stress. Changes in the Standardized Evaporative Stress Ratio (SESR) is commonly used to capture flash drought formation via evaporative stress within an ecosystem. SESR data was calculated for an area of Central North America that spans 20° - 60° N and 80° - 110° W, with SST and GPH at 30°S - 90°N and 0° - 180°W.

To analyze the composites presented in Chapter 3, SESR, SST, and 500 mb GPH was data was collected for the years that correspond to the flash drought years in the Southern Great Plains and Midwest localities presented in Table 3.1. To better understand the conditions leading to flash

drought, data variables were collected for the 30-day antecedent periods in conjunction with Chapter 3. These 30-day periods were then converted to pentad values representing 5-day means. In a similar process to SESR, SST and GPH were standardized and detrended to create a set of standardized anomalies.

To validate the SST and atmospheric pressure patterns identified in Chapter 3 and the temporal displacement to their impact on regional flash drought, this study will employ the Extended Empirical Orthogonal Function (EOF) method. EOF is a method to decompose a signal that varies in space and time, to interpret patterns of variability through time. It will result in Principal Component timeseries (PCs) that when projected onto the original SST, GPH, and SESR data respectively will offer the largest patterns (Modes) of co-variability within the system. An extended EOF contains multiple variables and can be used to introduce time deltas into the study to examine the effects of the propagation SST and atmospheric patterns onto changes of evaporative stress within the Central US. EOFs can be tricky as each mode is derived by and represents data, not necessarily a physical mode. The physical representation of an EOF mode is a matter of subjective interpretation (Bjornsson & Venegas, 1997). In climate studies the largest amount of variability is usually contained in the first few modes.

For the extended EOF analysis the three major datasets were collapsed into a single matrix with corresponding time (M) dimensions (72 pentads for the SGP and 48 pentads for the MW). Spatial points are collapsed into a vector with all variables appended to the end (N; 156144 datapoints with 64563, 86640, and 4941 representing SST, GPH, and SESR respectively). This results in matrix A, with M x N dimensions where vector (N) is moving through time (M). To ensure equal area weighting, the matrix is spatially weighted by multiplying the values by

$\sqrt{\cos(latitude)}$. The covariance (dispersion) matrix is calculated via equation 4.1. Where A represents the weighted data matrix, A^T is the transpose of A, and M is the time dimension of dataset. The resulting covariance matrix (C) has M x M dimensions.

$$\boldsymbol{C = \frac{1}{M} A^T A} \quad \textbf{4.1)}$$

Eigenvectors (e_1) are a 1 x N vector with the highest resemblance to the ensemble of state vectors. Eigenanalyzing through squaring and maximization each eigenvector of C is equivalent to that eigenvector with a corresponding amplitude (λ; eq. 4.2).

$$\boldsymbol{Ce_1 = \lambda e_1} \quad \textbf{4.2)}$$

These eigenvectors are the EOFs of matrix A with the largest λ values corresponding to EOF-1 and explaining the largest fraction of variance in matrix A. Projection of these derived eigenvectors onto the spatially weighted anomalies will calculate the principal timeseries (PCs) for the period of record (Bjornsson and Venegas, 1997). The fraction of variance explained by each EOF is calculated by equation 4.3.

$$\boldsymbol{\frac{\lambda_n}{\sum \lambda_n} * 100} \quad \textbf{4.3)}$$

The resulting EOFs/PCs are dimensionless. To present the data in a meaningful way, the original unweighted datasets are regressed onto the standardized PC time series for each mode. This regression will restore the original units of measurement to the data matrix. As this is a multivariable EOF the standardized PCs are regressed onto each SESR, SST, and GPH separately. Because remote drivers such as SST are far removed from the study areas, pentad temporal lags were introduced between SST and GPH with SESR. Lags varied from 0 pentads to

6 (0 to 30 days). To attempt to see the downstream effect that these teleconnections have on the local SESR values, lags were only introduced to the SESR data points. Both the M and N dimensions were preserved however the dates of the individual SESR datapoints were lagged.

Finally, both the lagged and unlagged PC timeseries were correlated with change in SESR data values and then subjected to a bootstrap simulation with N = 10000 iterations to assess statistical significance.

4.3 Results:

4.3.1 Southern Great Plains

The first three MODES of the extended EOF of flash drought years selected for the SGP (table 3.1) explain 37.3 % of the total variability between remote SSTs, GPHs, and SESR in the Central US. MODE 1, which holds the largest eigenvalues explains 22.1 % of the total variability. Regression of each variable onto the MODE 1 PC time series (Fig. 4.1) shows the spatial variance of each respective variable. Both the spatial representation of variance explained for SST and GPH closely resemble the patterns of standardized anomalies in the antecedent composite for the SGP in Chapter 3 (Fig. 3.2). An area of warm anomalies in the North Central Pacific is congruent with that found in Chapter 3 and corresponds to the region where Rossby wave packets during Central US flash drought years found by Jong et al. (2022). The tropical Pacific in MODE 1 differs from that of the composites with areas of warm anomalies off the West Coast of South America. Areas of Pacific SST anomalies that register as significant in Figure 3.2 do match with those in Figure 4.1 suggesting that these areas are crucial to driving changes in evaporative stress. Both high and low GPH anomalies are well represented, with a

ridge in the Central US. Warm SST anomalies also occur along the East Coast of the US, which closely correspond to SST anomalies in Figure 3.2. EOF 1 does not exhibit as much warming in

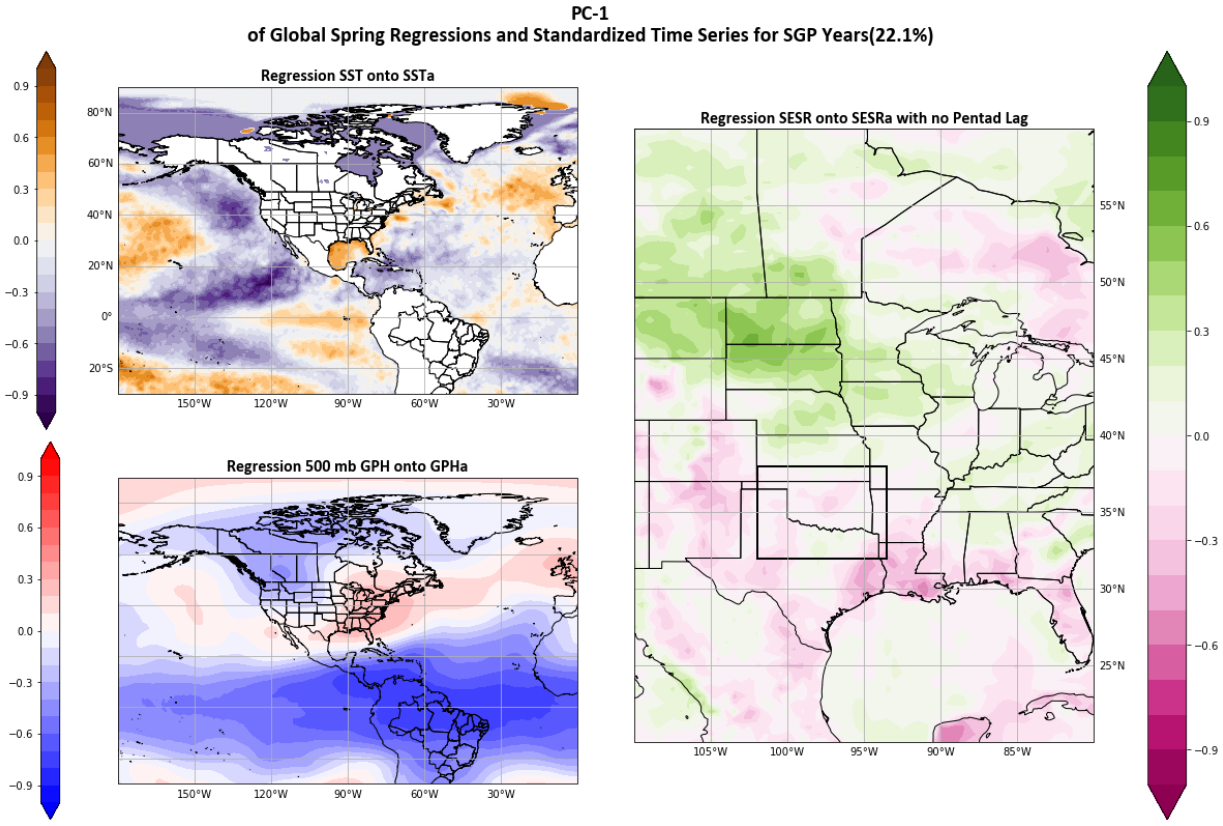

Figure 4.1 *Spatial representation of Principal Component time series MODE 1 regressed with standardized anomalies of a) SST, b) 500 mb GPH, and c) SESR for the Southern Great Plains flash drought years.*

the North Atlantic as the antecedent composite. However, GPH anomalies both for EOF mode 1 and Figure 3.2 exhibit an atmospheric ridge present over Central North America and large low GPH and SST anomalies over the Tropical Pacific.

Both the SST and GPH patterns are suggestive of La Nina pattern of ENSO (Rasmusson & Carpenter, 1982). The La Nina pattern brings drier warmer air to the SGP (Rasmusson & Carpenter, 1982; Flanagan et al., 2018; 2019) as moisture is shifted south with the tropical jet. Droughts are more common in the SGP during La Nina and the patterns in MODE 1 reinforce that La Nina patterns are driving some SGP flash drought events. EOF MODE 1 spatial SESR plot supports drying due to La Nina. Drying is occurring in the South-Central US, with moisture shifted to the north and south.

EOF MODE 2 (Fig. 4.2) also has some spatial resemblance to that of the SGP antecedent composite (Fig. 3.4). A band of high SST and GPH anomalies extends from the Central Pacific through the Southern US and into the Atlantic. This area corresponds to the anomalous easterly winds present in Figure 3.2b. MODE 2 patterns may be a result of anomalies that are associated with easterly winds associated with drier air. Although weaker, a ridge remains present over the Central US that corresponds to the increases of atmospheric demand associated with flash drought development (Basara et al., 2019; Jong et al., 2022; Chapter 3).

MODE 3 patterns more resemble the features in the SGP development composite (Fig. 3.6) but only represents 6.7 % of the variability and may correspond to variation temporally later in the datasets. Flash drought start dates were calculated via the methodology in Chapter 3. This method utilizes the mean start date in in the spatial area, which can allow for some bias and overlapping of the antecedent and development periods. Although the EOF analysis was only performed with the antecedent period, the possibility exists of biased results in MODE 3.

SESR variations in MODE 3 are dichotomous with increased atmospheric stress in the east and less in the west. This pattern matches closely to the soil moisture in Figure 3.3c and may

be a result of decreased atmospheric stress due to increased atmospheric moisture via evapotranspiration (Seneviratne et al., 2010).

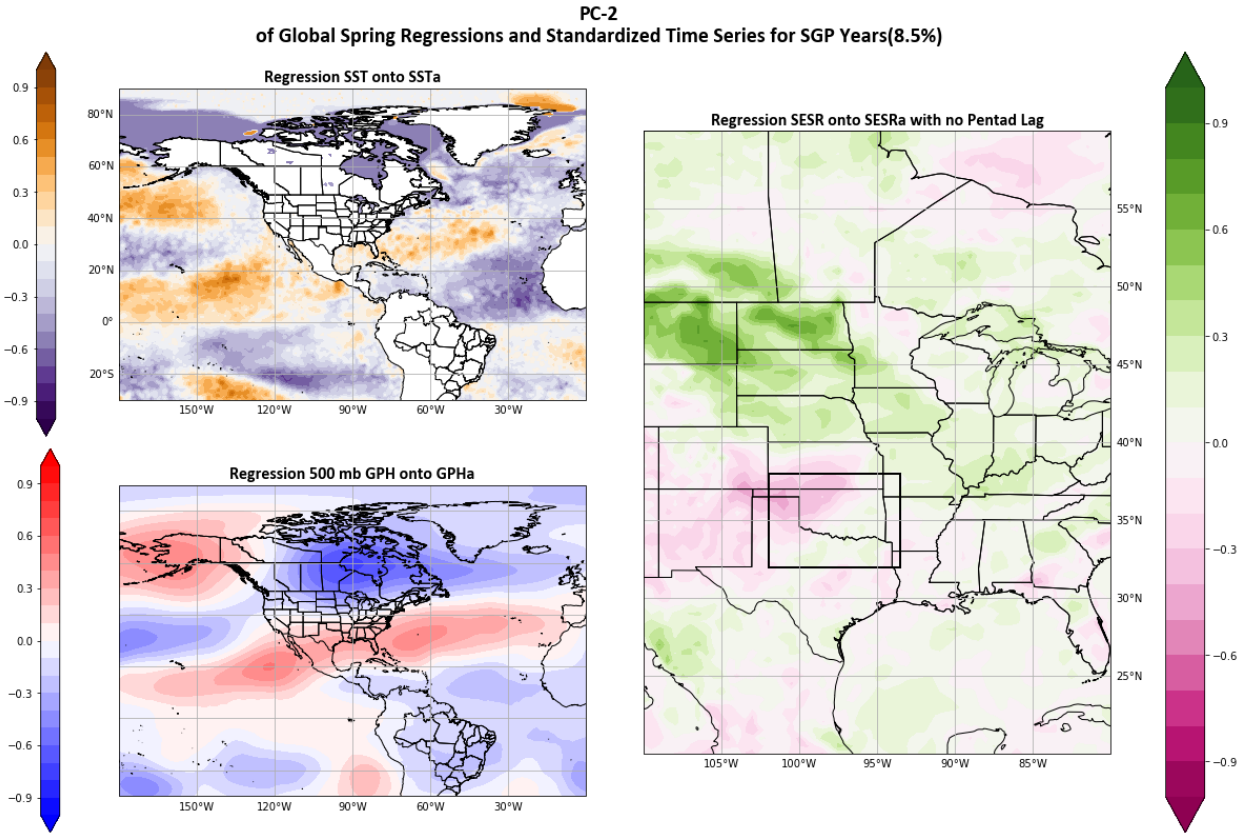

Figure 4.2 *Spatial representation of Principal Component time series MODE 2 regressed with standardized anomalies of a) SST, b) 500 mb GPH, and c) SESR during Southern Great Plains flash drought years.*

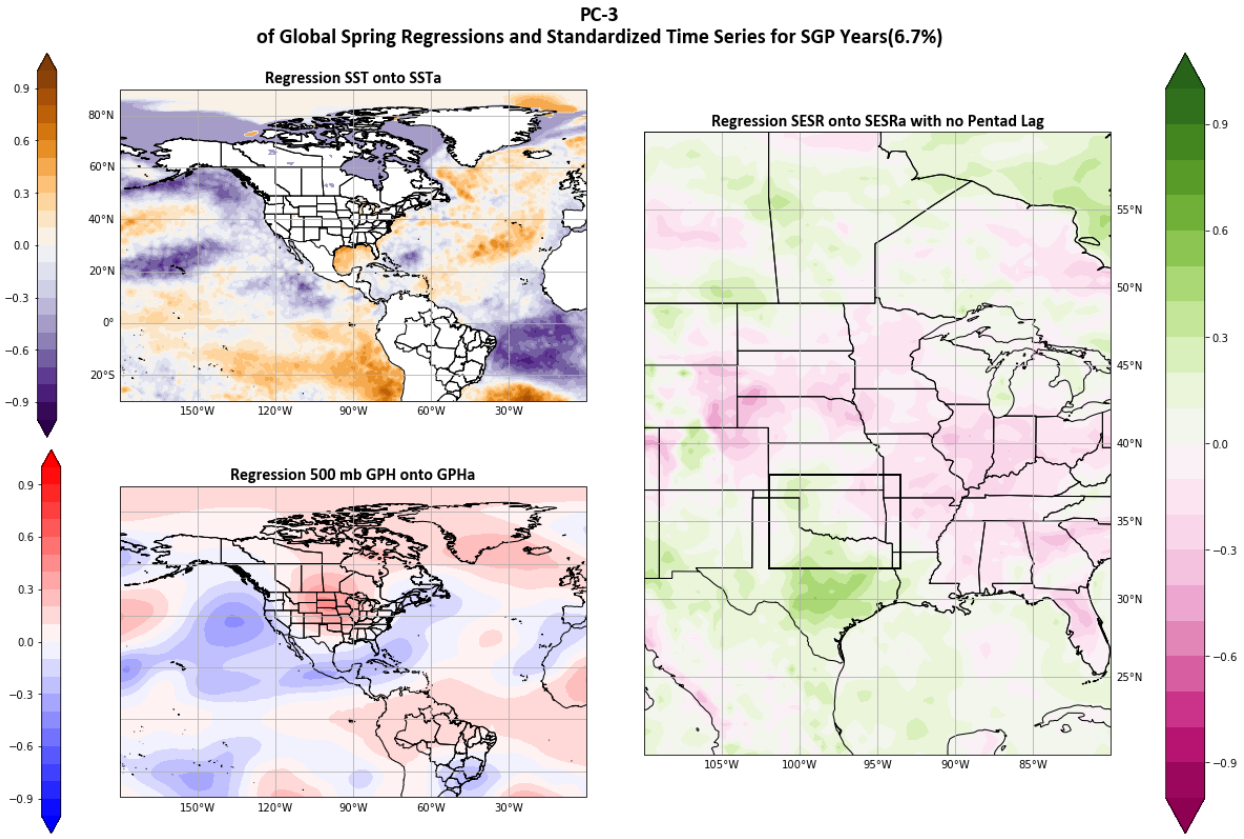

Figure 4.3 *Spatial representation of Principal Component time series MODE 2 regressed with standardized anomalies of a) SST, b) 500 mb GPH, and c) SESR during Southern Great Plains flash drought years.*

Correlation testing was completed between each of the first three PC MODES and decreases in SESR values within the SGP for the same temporal period. A bootstrap simulation was used to randomly sample the data 10,000 times and then correlations were calculated as a percentile (Table 4.1). Traditionally, significant values are registered above the 90th or 95th percentile. None of the PC MODES registered that level of significance. However, the first 2 MODES did register near to the 80th percentile at 81.08% and 79.44% for MODE 1 and MODE 2, respectively.

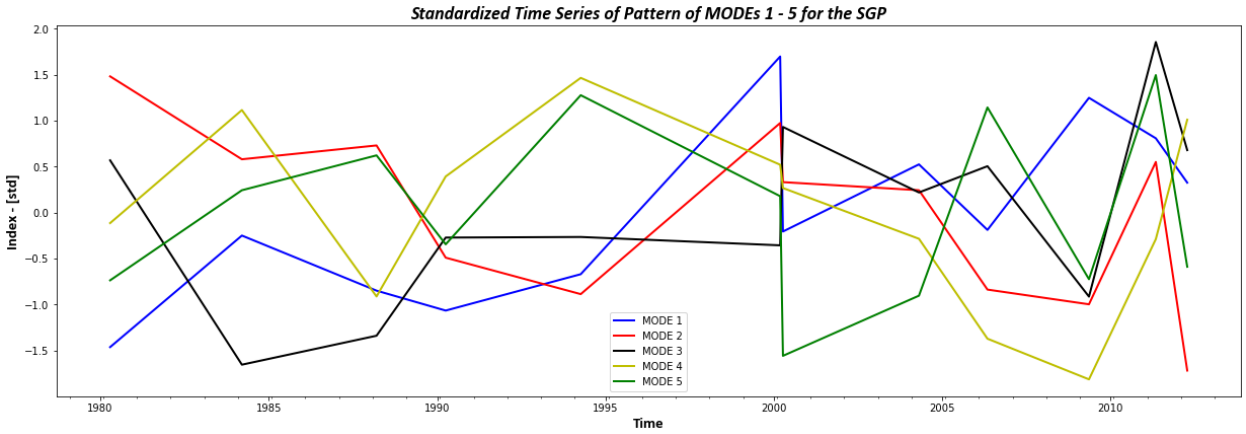

Figure 4.4 *PC time series of the first 5 MODES for the SGP region.*

Table 4.1 *Significance as a percentage as calculated via bootstrapping simulation methodology.*

	SGP			MW		
	MODE 1	MODE 2	MODE 3	MODE 1	MODE 2	MODE 3
No Lag	81.08	79.44	72.72	48.76	95.75	77.10
2 P Lag	66.40	57.46	76.34	65.42	88.58	83.04
3 P Lag	83.74	42.32	57.50	82.50	85.62	78.94
4 P Lag	65.52	42.42	41.97	63.46	85.53	83.26
5 P Lag	66.44	42.38	42.68	56.24	92.40	81.22

4.3.2 Midwest

Regression of SST onto PC MODE 1 for the MW (Fig. 4.3) is similar to the MW antecedent composite (Fig. 3.5) with SST anomalies in the Tropical Pacific that are cooler than expected based on the composite. However, a matching band of cooler SST anomalies are present near Central American that is accompanied by low GPH anomalies. An omega blocking pattern is also present. This pattern inhibits moisture from traveling over through the central blocking high

(Rex, 1950). The outer GPH high areas correspond to warm SST anomalies. In the North Central Pacific, the warm SST anomalies are similar to the significant SST anomalies from Figure 3.5. Again, this area is the area where Jong et al., (2022) found origination of Rossby wave packets that develop into stalled high atmospheric ridges over the Ohio Valley. Warm SST anomalies in the Atlantic could correspond to a positive NAO that has been found to increase the incidence of flash drought in the Midwest (Lesinger & Tian, 2022). Overall, the MODE 1 patterns are very consistent with conditions that are known to drive flash drought development in the Midwest.

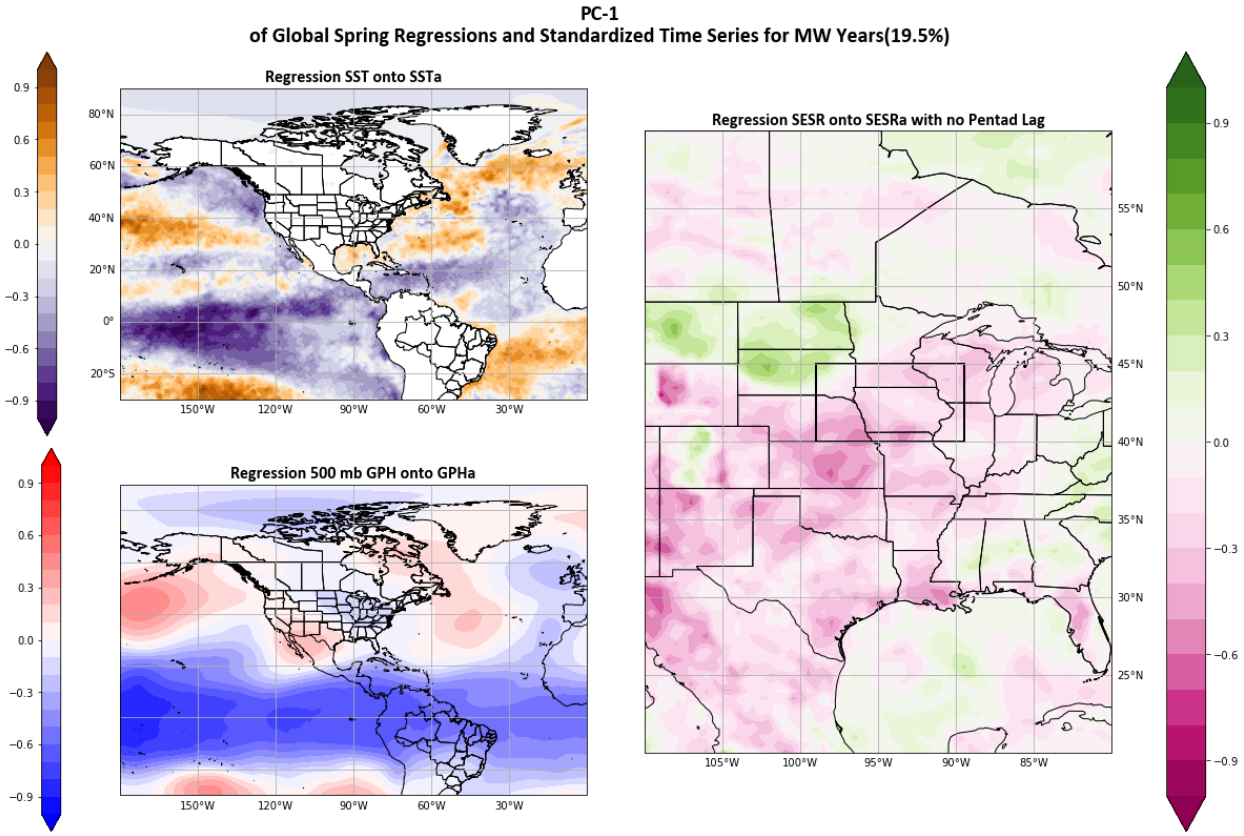

Figure 4.5 *Spatial representation of Principal Component time series MODE 1 regressed with standardized anomalies of a) SST, b) 500 mb GPH, and c) SESR for Midwest flash drought years.*

PC MODE 1 represents 19.5% of the total variance, with the first three standing for 41.3% of the total variability. PC MODE 2 only represents 12.5% of the total variance, but also registers as the most statistically significant when subjected to bootstrap simulation comparison with changes in evaporative stress. As such, MODE 2 for the MW tests at 95.75% while MODE 1 only at 48.76%despite some similarities in the spatial patterns. MODE 2 (Fig. 4.6) SST exhibits a strong El Nino style pattern in the Central Pacific (Rasmusson & Carpenter, 1982). El Nino is known for moisture transport to the Southern US and drier conditions to the Midwest (Rasmusson & Carpenter, 1982; Flanagan et al., 2018; 2019). Warm SST shifting to the coast of South America allows for the extension of the pacific jet into the Southwest US. While the North Central Pacific is cooler overall there is still a small area of warm SST anomalies, with a GPH high just to the south. GPH anomalies over the central US are neutral however evaporative stress increased in these areas. During significance testing MODE 2 tested as the most significant pattern relating to changes in evaporative stress in the associated study area at over the 95th percentile (Table 2).

Like MODE 2 for the SGP, MODE 3 for MW years resembles the development composite from Chapter 3 (Fig. 3.7). Rossby wave amplitude seems to have decreased with an increased frequency shown through several pairs of alternating GPH highs and lows. Again, this is likely bias via the methodology of flash drought identification. A ridge is present via the analysis over Western North America. Subsidence on the eastern side of the ridge causes increases in evaporative stress (Ford & Labosier, 2017; Jong et al., 2022; Chapter 3) shown in Figure 4.7.

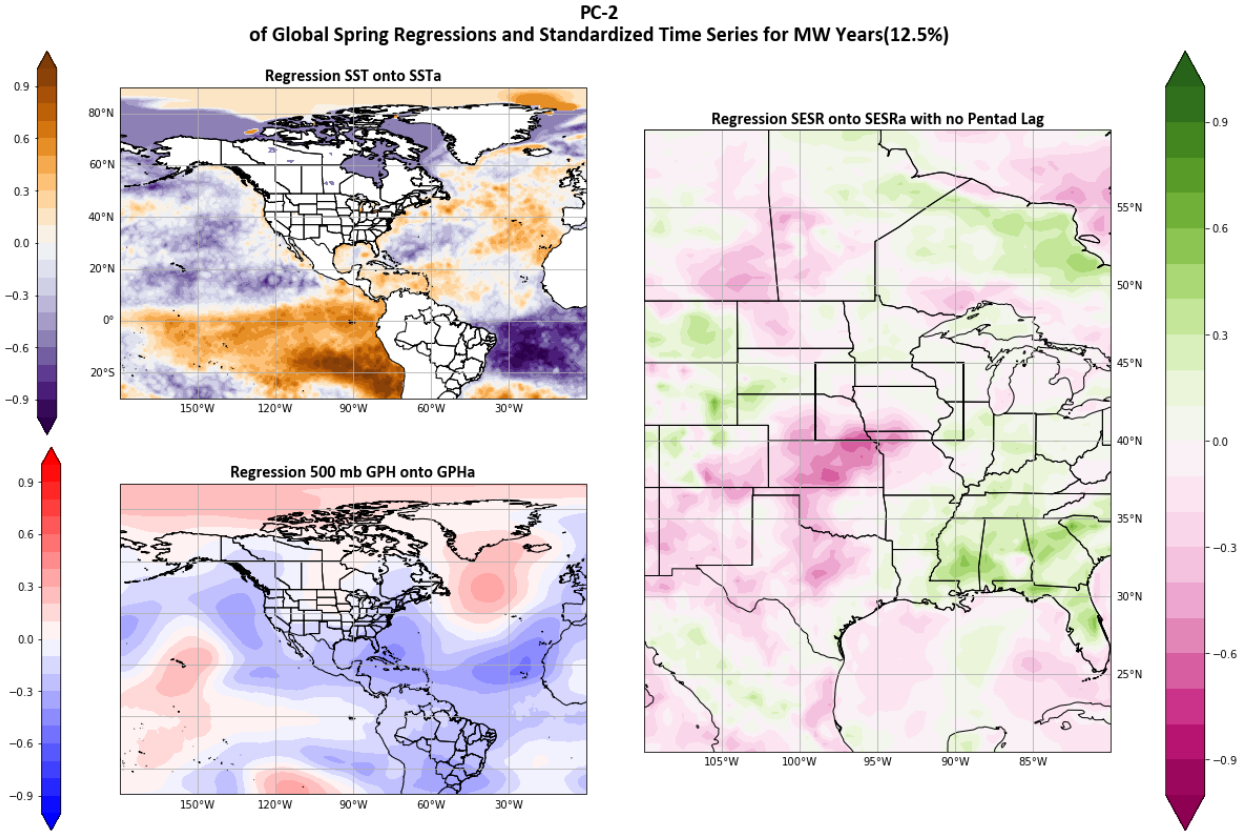

Figure 4.6 *Spatial representation of Principal Component time series MODE 2 regressed with standardized anomalies of a) SST, b) 500 mb GPH, and c) SESR for Midwest flash drought years.*

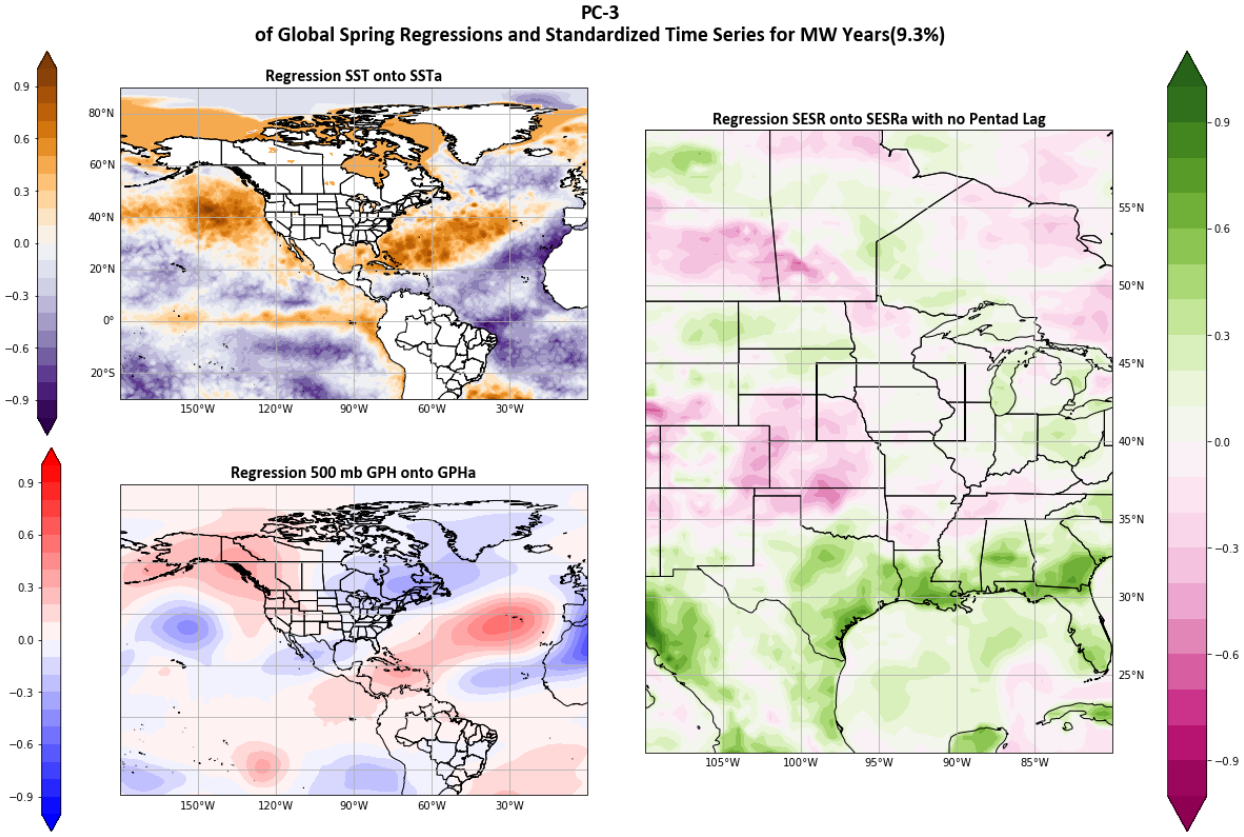

Figure 4.7 *Spatial representation of Principal Component time series MODE 3 regressed with standardized anomalies of a) SST, b) 500 mb GPH, and c) SESR for Midwest flash drought years.*

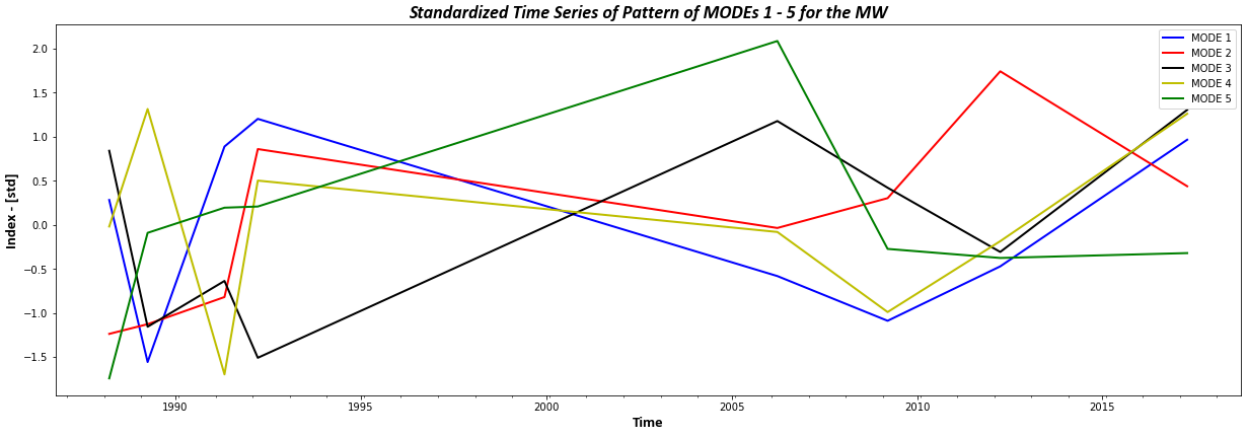

Figure 4.8 *PC time series of the first 5 MODES for the SGP region.*

Despite EOF analysis being strictly a mathematical process (Bjornsson & Venegas, 1997), patterns of variability in multiple PC timeseries show results consistent with previously found atmospheric patterns of flash drought development (Cook et al., 2022; Jong et al., 2022; Chapter 3). Remote SST oscillations appear in MODE 1 for both study regions. SST oscillations can increase the likelihood of flash drought development both within the SGP and the MW (Lesinger & Tian, 2022; Chapter 3). In all MODES tested in both study areas have GPH atmospheric patterns that represent ridging close to or directly over their respective study areas. High atmospheric ridging is essential to flash drought development through changes in evaporative stress (Otkin et al., 2014; 2018; Basara et al., 2019; Christian et al., 2019; 2021; 2024; Jong et al., 2022, Chapter 2; 3).

4.3.3 Lagged SESR Covariance Matrix

Spatial representations of EOF MODES of variability are subjective given the mathematical process and do not rely on physics (Dommenget & Latif, 2002; Bjornsson & Venegas, 1997). While a resemblance exists between the first 3 MODES of variability in both study regions, a lag analysis was conducted. Regression of SESR values on to the PCs with lag built into the covariance matrix varied little compared to the non-lagged analyses (often as little as $1/1000^{th}$ of a standardized deviation between lags). Spatially this created little difference between the plots. These results make it difficult to quantify any changes in evaporative stress despite remote teleconnections reflecting already identified drought patterns (Ford & Labosier, 2017; Jong et al., 2022; Chapter 3).

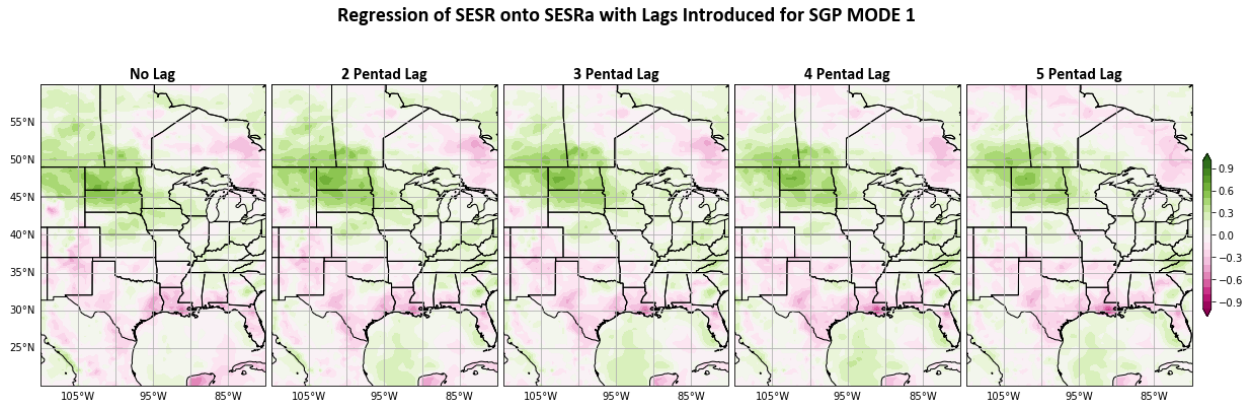

Figure 4.9 *Changes in Evaporative Stress when incrementally lagged SESR values are substituted in the covariance matrix.*

Figure 4.9 shows the changes in SESR values for each lagged pentad for MODE 1 in SGP drought years 4.10 in MW MODE 1 and 2. MW MODE 2 is included as it is the most statistically significant pattern. Neither spatial plot distinctly displays a noticeable difference in evaporative stress. Incremental increases of evaporative stress occur in the SGP region, however there are more noticeable increases outside the study area. The MW areas show slight decreases in overall evaporative stress through time, while there are larger increases in other regions of the US.

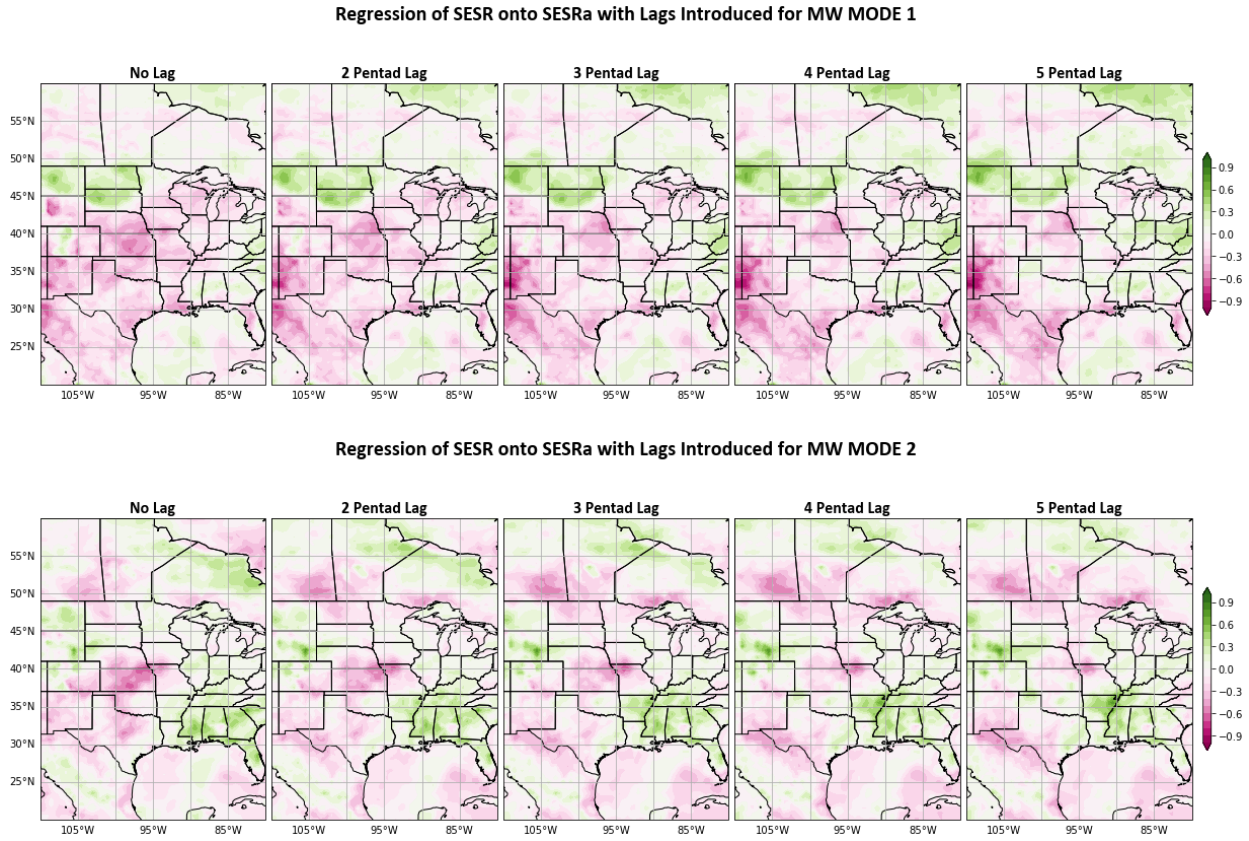

Figure 4.10 *Changes in Evaporative Stress when incrementally lagged SESR values are substituted in the covariance matrix for MODES 1 and 2.*

4.4 Conclusions:

Extended EOF analysis has reinforced previously found synoptic scale patterns associated with flash drought development (Jong et al., 2022; Lesinger & Tian, 2022; Chapter 3) that can help to better understand remote drivers. EOF itself is a mathematically based process that can only recognize patterns of co-variability. Even though EOF patterns do not represent physical processes the patterns found do represent parts of physical process that are known to drive

drought and flash drought within the Central US (Otkin et al., 2014; Ford & Labosier, 2017; Basara et al., 2019; Christian et al., 2019a; 2021; Parker et al., 2021; Cook et al., 2022; Jong et al., 2022; Chapter 2; Chapter 3).

Multiple MODES in both study areas are tied with SST oscillations that better tie SST variation directly to changes in evaporative stress. Also, these results have confirmed that warming in the North Central Pacific plays a role in atmospheric patterns that block moisture migration into the Central US (Jong et al., 2022) prior to both SGP and MW flash drought events.

Atmospheric GPH anomalies are congruent with SST anomalies and show well recognized drought driving conditions prior to flash droughts. This is most apparent in MODE 1 of MW years. A classic omega block pattern is present limiting moisture movement (Rex, 1950). This recognition of specific patterns of both remote SST and synoptic scale GPH anomalies that lead to increases of evaporative stress can lead to better methods of prediction. Many flash drought prediction attempts use changes in precipitation, evaporative stress or soil moisture. Addition of SST and GPH anomaly patterns can help to extend warning to possible changes in these variables that lead to cascading flash drought symptoms. The lack of impact adding lag to variables in this situation does not lend itself to bettering attempts at prediction. Because of flash droughts cascading intensification, prediction can be particularly challenging without better understanding of the temporal component between remote drivers and local changes. Building on these patterns that show consistency with previous results and composites, additional attempts to examine the lag between SST anomalies and local impacts should be addressed.

Chapter 5: Summary and Key Findings:

5.1 Overview:

Flash droughts have become an ever-increasing problem that threatens both food and water security globally. Flash drought predictability is challenging due not only to its seasonal to subseasonal temporal scale but also due to the multiple local, regional, and synoptic scale drivers that work in unison to drive them. Most attempts at flash drought prediction rely on local scale soil moisture, precipitation, and temperature fluxes. As precipitation is the known first order driver of drought, flash drought relies on additional drivers to initiate the cascading effects that result in rapid desiccation of ecosystems. The feedbacks between soil moisture, evapotranspiration and temperature is well documented (Seneviratne et al., 2010), however the interplay of these feedbacks on seasonal to subseasonal time periods is less so. To extend the temporal range of flash drought prediction capabilities these feedbacks need to be examined at longer temporal periods.

Some of the larger scale drivers of flash drought are also known. High atmospheric ridging has been linked to flash drought development (PaiMazdur & Done, 2016; Ford & Labosier 2017; Basara et al., 2019; Bolles et al., 2021; Jong et al., 2022; Kautz et al., 2022) and Rossby wave packets that cause ridges over the Ohio valley have been traced to the North Pacific (Jong et al., 2022). The forces that generate these wave packets and the atmospheric patterns that drive their propagation are unknown. Cyclic SST oscillations have also been shown to influence

drought in the US (Lesinger & Tian, 2022). However specific SST, GPH, and zonal wind anomalies that drive flash drought have not been studied in depth.

To help to further the ability of flash drought prediction on a longer temporal scale the purpose of this research is to prove that the current suite of environmental products is sufficient to 1) understand temporal influences of atmosphere on soil moisture to identify regions that may be primed for flash drought through seasonal to subseasonal fluxes, 2) assess SST teleconnections and synoptic scale atmospheric processes that work in concert with local systems to drive flash drought and, 3) confirm the validity of the SST and synoptic scale processes mathematically through extended empirical orthogonal function analysis.

5.2 Key Findings and Future Work:

The complex relationships between land and atmosphere make attempts to predict flash drought challenging. Chapter 2 was aimed at identifying areas that are primed for flash drought development using seasonal trends of temperature and evaporative stress. Soil moisture is often used to track flash drought propagation (Ford et al., 2015; Bajgain et al., 2017; Chatterjee et al., 2022) and as such was used as a proxy for flash drought development. Seasonal temperatures and evaporative stress significantly impact the root zone soil moisture in the subsequent season. Evaporative stress is the greatest factor in soil moisture changes inter-seasonally and is found to be statistically significant for most of the continent. Multiple case studies of major flash droughts in Europe exhibited these seasonal trends in the months leading up to flash drought onset validating the utility of using this method to identify areas that are primed for development.

These findings linked lagged seasonal responses of soil moisture to atmospheric stresses. The methodology used to identify areas primed for flash drought relies on broad temporal ranges. Implementation of the same methodology with shorter or rolling temporal spans would offer better indication of specific time lags between atmospheric stress and soil moisture changes. Lag times may be specific to the region based on soil properties, however longer prediction timespans and better preparation can be achieved with increased understanding. Testing of this methodology with another evaporative stress metric such as the Rapid Change Index (Otkin et al., 2014) or Evaporative Demand Drought Index (Hobbins et al., 2016) may offer more insight into the exact nature of the land-atmosphere relationship.

Evaporative stress is a major driver of flash drought but the larger atmospheric drivers and oceanic teleconnections that lead to increases of evaporative stress are less understood. Knowing that seasonal evaporative stress can have a major impact on soil moisture, Chapter 3 focused on identifying synoptic scale patterns of sea surface temperature, geopotential height, and meridional wind anomalies that would lead to regional early year flash drought development. Composite plots of conditions prior to flash drought found that sea surface temperature oscillations associated with El Nino Southern Oscillation in the tropical Pacific and warming trends in the North Atlantic both contribute to flash drought development in the Central United States. Anomalous warming in the North Central Pacific also plays a significant role as it generates geopotential height anomalies and Rossby wave packets that create high atmospheric ridges. Subsidence to the east of these ridges contributes to increased evaporative stress and drying of the landscape. Composites of land surface variables at local scales identified that it can be difficult to predict flash drought using precipitation and soil moisture. Pre-drought levels of moisture were found to be high in both localities.

Few previous studies have focused on larger scale processes that lead to flash drought development versus specific variables of precipitation, evaporation, and soil moisture deficits (Lisonbee et al., 2022). Sea surface temperature oscillations have been associated with increases in flash drought likelihood (Lesinger & Tian, 2022) but those oscillations have not been connected to atmospheric changes specific to flash drought. Previously unknown North Central Pacific sea surface temperature anomalies identified in Chapter 3 connect with known atmospheric patterns that drive Central US flash droughts (Jong et al., 2022). These findings were validated in Chapter 4 through EOF analysis. Further examination of the North Pacific temperature anomalies and their influence in flash drought development can contribute to increased predictive model skill.

Atmospheric patterns through the development of flash drought confirmed that stalled high atmospheric ridges are present during flash droughts (Ford & Labosier, 2017; Basara et al., 2019; Jong et al., 2022). Changes in Rossby wave amplitudes and frequencies, in concert with changes in high atmospheric wind, promoted slowing of the wave packets thus inhibiting moisture migration. Identification of these larger synoptic scale processes present opportunities to use current datasets to create better predictive systems.

Local drivers of flash drought reach a tipping point where a cascade effect of feedbacks lead to quick soil desiccation. Soil moisture deficits are sometimes linked to flash drought development (Ford et al., 2015) however, results in Chapter 3 show that soil moisture surplus is more significant to flash drought development. This reinforces previous studies that show flash droughts can occur with little warning (Osman et al., 2022; Bolles et al., 2021; Otkin et al.,

2018b; Hoerling et al., 2014). Soil moisture surpluses or deficits may play a more significant role regionally.

To further evaluate the validity of the sea surface temperature and atmospheric patterns identified antecedent to flash drought, Chapter 4 examines the covariance of these synoptic scale processes with Central US evaporative stress. Extended Empirical Orthogonal Function (EOF) analysis was used to find the largest MODEs of co-variability within the combined system. Spatial representations of MODE 1 of the EOF analysis closely resembled the antecedent composites created in Chapter 3, confirming the impacts of these sea surface and atmospheric patterns on changes in evaporative stress in the Central US. Testing showed for Southern Great Plains droughts, MODE 1 sea surface temperature and atmospheric patterns correlated the best with increases of evaporative stress. For the Midwest MODE 2 is well correlated with increases of stress. While these specific patterns only represent a small percentage of the covariation of the three datasets, their specific relationship with changes in evaporative stress can be explored further.

Attempts to identify lag times between sea surface temperature, atmospheric, and evaporative stress anomalies were less successful. Introduction of incremental 5-day (pentad) lags into the EOF created little change in registered evaporative stress levels. This is likely due to the methodology used. Further exploration of the lag times with different methods is certainly warranted. Quantification of the temporal span from teleconnections to flash drought events will be key to relating to longer term seasonal to subseasonal prediction of flash droughts.

In a broad sense, the novel findings in this dissertation contribute to the understanding of synoptic and regional scale processes that drive flash drought. Connections between SST, zonal

winds, and GPH anomalies that lead to atmospheric ridge formation over the Central US can contribute to increased seasonal to subseasonal predictive skill. Although, continued study of these processes is necessary to better improve prediction methods (Pendergrass et al., 2020; Otkin et al., 2022). Identification of these teleconnections that help to drive changes in evaporative stress can extend the lead times for predictions. As flash drought is a global phenomenon, global teleconnection identifications are vital to understanding flash drought development in other regions. With continued global warming flash drought occurrence is predicted to increase (Christian et al., 2023; Black, 2024). Prediction models that include sea surface temperature changes and oscillations can give longer lead times that changes in precipitation and evaporative stress will occur increasing preparedness.

References:

(Eds.)., S. D. N. C. f. A. R. S. (Last modified 22 Jul 2013). *"The Climate Data Guide: Empirical Orthogonal Function (EOF) Analysis and Rotated EOF Analysis."*. NCAR. Retrieved 21 March from

Allen, R. G., Pereira, L. S., Raes, D., & Smith, M. (1998). Crop evapotranspiration-Guidelines for computing crop water requirements-FAO Irrigation and drainage paper 56. *Fao, Rome*, *300*(9), D05109.

Anderson, M. C., Hain, C., Otkin, J., Zhan, X., Mo, K., Svoboda, M., . . . Pimstein, A. (2013). An Intercomparison of Drought Indicators Based on Thermal Remote Sensing and NLDAS-2 Simulations with U.S. Drought Monitor Classifications. *Journal of hydrometeorology*, *14*(4), 1035-1056. https://doi.org/10.1175/JHM-D-12-0140.1

Azorin Molina, C., Vicente Serrano, S. M., Sanchez Lorenzo, A., McVicar, T. R., Moran Tejeda, E., Revuelto, J., . . . Tomas-Burguera, M. (2015). Atmospheric evaporative demand observations, estimates and driving factors in Spain (1961-2011). *Journal of hydrology (Amsterdam)*, *523*, 262-277. https://doi.org/10.1016/j.jhydrol.2015.01.046

Bador, M., Terray, L., & Boé, J. (2016). Emergence of human influence on summer record-breaking temperatures over Europe. *Geophysical research letters*, *43*(1), 404-412. https://doi.org/10.1002/2015GL066560

Bador, M., Terray, L., Boé, J., Somot, S., Alias, A., Gibelin, A.-L., & Dubuisson, B. (2016). Future summer mega-heatwave and record-breaking temperatures in a warmer France climate. *Environmental research letters*, *12*(7), 74025. https://doi.org/10.1088/1748-9326/aa751c

Bajgain, R., Xiao, X., Basara, J., Wagle, P., Zhou, Y., Zhang, Y., & Mahan, H. (2017). Assessing agricultural drought in summer over Oklahoma Mesonet sites using the water-related vegetation index from MODIS. *International journal of biometeorology*, *61*(2), 377-390. https://doi.org/10.1007/s00484-016-1218-8

Barker, L. J., Hannaford, J., Chiverton, A., & Svensson, C. (2016). From meteorological to hydrological drought using standardised indicators. *Hydrology and earth system sciences*, *20*(6), 2483-2505. https://doi.org/10.5194/hess-20-2483-2016

Basara, J. B., Christian, J. I., Wakefield, R. A., Otkin, J. A., Hunt, E. H., & Brown, D. P. (2019). The evolution, propagation, and spread of flash drought in the Central United States during 2012. *Environmental research letters*, *14*(8), 84025. https://doi.org/10.1088/1748-9326/ab2cc0

Basara, J. B., Maybourn, J. N., Peirano, C. M., Tate, J. E., Brown, P. J., Hoey, J. D., & Smith, B. R. (2013). Drought and Associated Impacts in the Great Plains of the United States°™A

Review. *International Journal of Geosciences*, *Vol.04No.06*, 10, Article 36204. https://doi.org/10.4236/ijg.2013.46A2009

Becker, E. (2023). *What we talk about when we talk about the jet stream and El Nino*. NOAA. Retrieved Mar. 27 from https://www.climate.gov/news-features/blogs/what-we-talk-about-when-we-talk-about-jet-stream-and-el-nino

Bjornsson, H., & Venegas, S. A. (1997). A manual for EOF and SVD analyses of climactic data. In (pp. 112 - 134). CCGCR Report 97.1.

Black, E. (2024). Global Change in Agricultural Flash Drought over the 21st Century. *Advances in atmospheric sciences*, *41*(2), 209-220. https://doi.org/10.1007/s00376-023-2366-5

Bolles, K. C., Williams, A. P., Cook, E. R., Cook, B. I., & Bishop, D. A. (2021). Tree-ring reconstruction of the atmospheric ridging feature that causes flash drought in the central United States since 1500. *Geophysical research letters*, *48*(4), n/a. https://doi.org/10.1029/2020GL091271

Buckley, T. N. (2019). How do stomata respond to water status? *The New phytologist*, *224*(1), 21-36. https://doi.org/10.1111/nph.15899

Buntgen, U., Urban, O., Krusic, P. J., Rybnicek, M., Kolar, T., Kyncl, T., . . . Trnka, M. (2021). Recent European drought extremes beyond Common Era background variability. *Nature geoscience*, *14*(4), 190-196. https://doi.org/10.1038/s41561-021-00698-0

Cassou, C. (2008). Intraseasonal interaction between the Madden-Julian Oscillation and the North Atlantic Oscillation. *Nature*, *455*(7212), 523-527. https://doi.org/10.1038/nature07286

Chatterjee, S., Desai, A. R., Zhu, J., Townsend, P. A., & Huang, J. (2022). Soil moisture as an essential component for delineating and forecasting agricultural rather than meteorological drought. *Remote sensing of environment*, *269*, 112833. https://doi.org/10.1016/j.rse.2021.112833

Chen, L. G., Hartman, A., Pugh, B., Gottschalck, J., & Miskus, D. (2020). Real-Time Prediction of Areas Susceptible to Flash Drought Development. *Atmosphere*, *11*(10), 1114. https://doi.org/10.3390/atmos11101114

Christian, J., Grace, T., Fellman, B., Mesheske, D., Edris, S., Olayiwola, H., . . . Furtado, J. (Exp. 2024). The Flash Droughts Across the South-Central United States in 2022: Drivers, Predictability, and Impacts. In. Submitted to Weather and Climate Extremes.

Christian, J. I., Basara, J. B., Hunt, E. D., Otkin, J. A., Furtado, J. C., Mishra, V., . . . Randall, R. M. (2021). Global distribution, trends, and drivers of flash drought occurrence. *Nature communications*, *12*(1), 6330-6330. https://doi.org/10.1038/s41467-021-26692-z

Christian, J. I., Basara, J. B., Hunt, E. D., Otkin, J. A., & Xiao, X. (2020). Flash drought development and cascading impacts associated with the 2010 Russian heatwave. *Environmental research letters*, *15*(9), 94078. https://doi.org/10.1088/1748-9326/ab9faf

Christian, J. I., Basara, J. B., Lowman, L. E. L., Xiao, X., Mesheske, D., & Zhou, Y. (2022). Flash drought identification from satellite-based land surface water index. *Remote Sensing Applications: Society and Environment*, *26*, 100770. https://doi.org/https://doi.org/10.1016/j.rsase.2022.100770

Christian, J. I., Basara, J. B., Otkin, J. A., & Hunt, E. D. (2019). Regional characteristics of flash droughts across the United States. *Environmental Research Communications*, *1*(12), 125004. https://doi.org/10.1088/2515-7620/ab50ca

Christian, J. I., Basara, J. B., Otkin, J. A., Hunt, E. D., Wakefield, R. A., Flanagan, P. X., & Xiao, X. (2019). A Methodology for Flash Drought Identification: Application of Flash Drought Frequency across the United States. *Journal of hydrometeorology*, *20*(5), 833-846. https://doi.org/10.1175/JHM-D-18-0198.1

Christian, J. I., Martin, E. R., Basara, J. B., Furtado, J. C., Otkin, J. A., Lowman, L. E. L., . . . Xiao, X. (2023). Global projections of flash drought show increased risk in a warming climate. *Communications earth & environment*, *4*(1), 165-110. https://doi.org/10.1038/s43247-023-00826-1

Cong, N., Wang, T., Nan, H., Ma, Y., Wang, X., Myneni, R. B., & Piao, S. (2013). Changes in satellite-derived spring vegetation green-up date and its linkage to climate in China from 1982 to 2010: a multimethod analysis. *Global change biology*, *19*(3), 881-891. https://doi.org/10.1111/gcb.12077

Cook, B. I., Williams, A. P., & Marvel, K. (2022). Projected changes in early summer ridging and drought over the Central Plains. *Environmental research letters*, *17*(10), 104020. https://doi.org/10.1088/1748-9326/ac8e1a

Dirmeyer, P. A., Koster, R. D., & Guo, Z. (2006). Do Global Models Properly Represent the Feedback between Land and Atmosphere? *Journal of hydrometeorology*, *7*(6), 1177-1198. https://doi.org/10.1175/JHM532.1

Dommenget, D., & Latif, M. (2002). A Cautionary Note on the Interpretation of EOFs. *Journal of climate*, *15*(2), 216-225. https://doi.org/10.1175/1520-0442(2002)015<0216:acnoti>2.0.co

2

Donat, M. G., Pitman, A. J., & Seneviratne, S. I. (2017). Regional warming of hot extremes accelerated by surface energy fluxes. *Geophysical research letters*, *44*(13), 7011-7019. https://doi.org/10.1002/2017GL073733

Edris, S. G., Basara, J. B., Christian, J. I., Hunt, E. D., Otkin, J. A., Salesky, S. T., & Illston, B. G. (2023). Analysis of the critical components of flash drought using the standardized evaporative stress ratio. *Agricultural and forest meteorology*, *330*, 109288. https://doi.org/10.1016/j.agrformet.2022.109288

Everitt, B. (2010). *The Cambridge dictionary of statistics / B.S. Everitt, A. Skrondal* (4th . ed.). Cambridge, UK ; New York : Cambridge University Press.

Fellman, B. (2023). Abrupt Agricultural Flash Drought: An Investigation of Rapid Drought Development Across Vital Agricultural Zones of the United States.

Fischer, E. M., Seneviratne, S. I., Vidale, P. L., LÜThi, D., & SchÄR, C. (2007). Soil Moisture–Atmosphere Interactions during the 2003 European Summer Heat Wave. *Journal of climate*, *20*(20), 5081-5099. https://doi.org/10.1175/JCLI4288.1

Flanagan, P. X., Basara, J. B., Furtado, J. C., Martin, E. R., & Xiao, X. (2019). Role of Sea Surface Temperatures in Forcing Circulation Anomalies Driving U.S. Great Plains Pluvial Years. *Journal of climate*, *32*(20), 7081-7100. https://doi.org/10.1175/JCLI-D-18-0726.1

Flanagan, P. X., Basara, J. B., Furtado, J. C., & Xiao, X. (2018). Primary Atmospheric Drivers of Pluvial Years in the United States Great Plains. *Journal of hydrometeorology*, *19*(4), 643-658. https://doi.org/10.1175/JHM-D-17-0148.1

Ford, T. W., & Labosier, C. F. (2017). Meteorological conditions associated with the onset of flash drought in the Eastern United States. *Agricultural and forest meteorology*, *247*, 414-423. https://doi.org/10.1016/j.agrformet.2017.08.031

Ford, T. W., McRoberts, D. B., Quiring, S. M., & Hall, R. E. (2015). On the utility of in situ soil moisture observations for flash drought early warning in Oklahoma, USA: SOIL MOISTURE DROUGHT EARLY WARNING. *Geophysical research letters*, *42*(22), 9790-9798. https://doi.org/10.1002/2015GL066600

Geng, G., Wu, J., Wang, Q., Lei, T., He, B., Li, X., . . . Liu, D. (2016). Agricultural drought hazard analysis during 1980–2008: a global perspective. *International journal of climatology*, *36*(1), 389-399. https://doi.org/10.1002/joc.4356

Gudmundsson, L., & Seneviratne, S. I. (2016). Anthropogenic climate change affects meteorological drought risk in Europe. *Environmental research letters*, *11*(4), 44005-44012. https://doi.org/10.1088/1748-9326/11/4/044005

Hari, V., Rakovec, O., Markonis, Y., Hanel, M., & Kumar, R. (2020). Increased future occurrences of the exceptional 2018–2019 Central European drought under global warming. *Scientific reports*, *10*(1). https://doi.org/10.1038/s41598-020-68872-9

Haskett, J. D. (2022). Intergovernmental panel on climate change : sixth assessment report / Jonathan D. Haskett.

Hobbins, M., Wood, A., Streubel, D., & Werner, K. (2012). What Drives the Variability of Evaporative Demand across the Conterminous United States? *Journal of hydrometeorology*, *13*(4), 1195-1214. https://doi.org/10.1175/JHM-D-11-0101.1

Hobbins, M. T., Wood, A., McEvoy, D. J., Huntington, J. L., Morton, C., Anderson, M., & Hain, C. (2016). The Evaporative Demand Drought Index. Part I: Linking Drought Evolution to Variations in Evaporative Demand. *Journal of hydrometeorology*, *17*(6), 1745-1761. https://doi.org/10.1175/JHM-D-15-0121.1

Hoerling, M., Eischeid, J., Kumar, A., Leung, R., Mariotti, A., Mo, K., . . . Seager, R. (2014). CAUSES AND PREDICTABILITY OF THE 2012 GREAT PLAINS DROUGHT. *Bulletin of the American Meteorological Society*, *95*(2), 269-282. https://doi.org/10.1175/BAMS-D-13-00055.1

Hoy, A., Hänsel, S., Skalak, P., Ustrnul, Z., & Bochníček, O. (2017). The extreme European summer of 2015 in a long-term perspective. *International journal of climatology*, *37*(2), 943-962. https://doi.org/10.1002/joc.4751

Ionita, M., Tallaksen, L. M., Kingston, D. G., Stagge, J. H., Laaha, G., Lanen, V. H. A. J., . . . Haslinger, K. (2017). The European 2015 drought from a climatological perspective. *Hydrology and earth system sciences*, *21*(3), 1397-1419. https://doi.org/10.5194/hess-21-1397-2017

Jensen, J. R. (2007). Remote sensing of the environment : an earth resource perspective / John R. Jensen.

Jiao, W., Wang, L., Smith, W. K., Chang, Q., Wang, H., & D'Odorico, P. (2021). Observed increasing water constraint on vegetation growth over the last three decades. *Nature communications*, *12*(1), 3777-3777. https://doi.org/10.1038/s41467-021-24016-9

Jin, C., Luo, X., Xiao, X., Dong, J., Li, X., Yang, J., & Zhao, D. (2019). The 2012 Flash Drought Threatened US Midwest Agroecosystems. *Chinese geographical science*, *29*(5), 768-783. https://doi.org/10.1007/s11769-019-1066-7

Jong, B.-T., Newman, M., & Hoell, A. (2022). Subseasonal Meteorological Drought Development over the Central United States during Spring. *Journal of climate*, *35*(8), 2525-2547. https://doi.org/10.1175/JCLI-D-21-0435.1

Kautz, L.-A., Martius, O., Pfahl, S., Pinto, J. G., Ramos, A. M., Sousa, P. M., & Woollings, T. (2022). Atmospheric blocking and weather extremes over the Euro-Atlantic sector – a review. *Weather and Climate Dynamics*, *3*(1), 305-336. https://doi.org/10.5194/wcd-3-305-2022

Lakshmi, V., Piechota, T., Narayan, U., & Tang, C. (2004). Soil moisture as an indicator of weather extremes: SOIL MOISTURE CLIMATE EXTREMES. *Geophysical research letters*, *31*(11), n/a. https://doi.org/10.1029/2004GL019930

Lawrence, D. M., Thornton, P. E., Oleson, K. W., & Bonan, G. B. (2007). The Partitioning of Evapotranspiration into Transpiration, Soil Evaporation, and Canopy Evaporation in a GCM: Impacts on Land–Atmosphere Interaction. *Journal of hydrometeorology*, *8*(4), 862-880. https://doi.org/10.1175/JHM596.1

Lesinger, K., & Tian, D. (2022). Trends, variability, and drivers of flash droughts in the contiguous United States. *Water resources research*, *58*(9), n/a. https://doi.org/10.1029/2022WR032186

Li, W., Migliavacca, M., Forkel, M., Denissen Jasper, M. C., Reichstein, M., Yang, H., . . . Orth, R. (2022). Widespread increasing vegetation sensitivity to soil moisture. *Nature communications*, *13*(1), 1-9. https://doi.org/10.1038/s41467-022-31667-9

Li, W., Migliavacca, M., Forkel, M., Walther, S., Reichstein, M., & Orth, R. (2021). Revisiting global vegetation controls using multi-layer soil moisture. *Geophysical research letters*, *48*(11), n/a. https://doi.org/10.1029/2021GL092856

Lisonbee, J., Woloszyn, M., & Skumanich, M. (2022). Making Sense of Flash Drought: Definitions, Indicators, and Where We Go From Here. *Journal of Applied and Service Climatology*, *Volume 2022*(001). https://doi.org/DOI : https://doi.org/10.46275/JOASC.2021.02.001

Liu, X., He, B., Guo, L., Huang, L., & Chen, D. (2020). Similarities and Differences in the Mechanisms Causing the European Summer Heatwaves in 2003, 2010, and 2018. *Earth's future*, *8*(4), n/a. https://doi.org/10.1029/2019EF001386

Liu, X., Zhu, X., Pan, Y., Li, S., Liu, Y., & Ma, Y. (2016). Agricultural drought monitoring：Progress, challenges, and prospects. *Journal of geographical sciences*, *26*(6), 750-767. https://doi.org/10.1007/s11442-016-1297-9

Lorenz, D. J., Otkin, J. A., Svoboda, M., Hain, C. R., & Zhong, Y. (2018). Forecasting Rapid Drought Intensification Using the Climate Forecast System (CFS). *Journal of geophysical research. Atmospheres*, *123*(16), 8365-8373. https://doi.org/10.1029/2018JD028880

Luterbacher, J., Dietrich, D., Xoplaki, E., Grosjean, M., & Wanner, H. (2004). European seasonal and annual temperature variability, trends, and extremes since 1500. *Science (American Association for the Advancement of Science)*, *303*(5663), 1499-1503. https://doi.org/10.1126/science.1093877

Ma, R., & Yuan, X. (2023). Subseasonal Ensemble Prediction of Flash Droughts over China. *Journal of hydrometeorology*, *24*(5), 897-910. https://doi.org/10.1175/JHM-D-22-0150.1

Ma, Z., Yan, N., Wu, B., Stein, A., Zhu, W., & Zeng, H. (2019). Variation in actual evapotranspiration following changes in climate and vegetation cover during an ecological restoration period (2000–2015) in the Loess Plateau, China. *The Science of the total environment*, *689*, 534-545. https://doi.org/10.1016/j.scitotenv.2019.06.155

Marchin, R. M., Backes, D., Ossola, A., Leishman, M. R., Tjoelker, M. G., & Ellsworth, D. S. (2022). Extreme heat increases stomatal conductance and drought-induced mortality risk in vulnerable plant species. *Global change biology*, *28*(3), 1133-1146. https://doi.org/10.1111/gcb.15976

Miralles, D., Teuling, A. J., Heerwaarden, v. C. C., & Vilà-Guerau de Arellano, J. (2014). Mega-heatwave temperatures due to combined soil desiccation and atmospheric heat accumulation. *Nature geoscience*, *7*(5), 345-349. https://doi.org/10.1038/ngeo2141

Miralles, D. G., Gentine, P., Seneviratne, S. I., & Teuling, A. J. (2019). Land–atmospheric feedbacks during droughts and heatwaves : state of the science and current challenges. *Annals of the New York Academy of Sciences*, *1436*(1), 19-35. https://doi.org/10.1111/nyas.13912

Miralles, D. G., van den Berg, M. J., Teuling, A. J., & de Jeu, R. A. M. (2012). Soil moisture-temperature coupling: A multiscale observational analysis. *Geophysical research letters*, *39*(21), n/a. https://doi.org/10.1029/2012GL053703

Mo, K. C., & Lettenmaier, D. P. (2016). Precipitation Deficit Flash Droughts over the United States. *Journal of hydrometeorology*, *17*(4), 1169-1184. https://doi.org/10.1175/JHM-D-15-0158.1

Mukherjee, S., & Mishra, A. K. (2022). Global Flash Drought Analysis: Uncertainties From Indicators and Datasets. *Earth's future*, *10*(6), n/a. https://doi.org/10.1029/2022EF002660

Mukherjee, S., Mishra, A. K., Ashfaq, M., & Kao, S.-C. (2022). Relative effect of anthropogenic warming and natural climate variability to changes in Compound drought and heatwaves. *Journal of hydrology (Amsterdam)*, *605*(C), 127396. https://doi.org/10.1016/j.jhydrol.2021.127396

Naumann, G., Cammalleri, C., Mentaschi, L., & Feyen, L. (2021). Increased economic drought impacts in Europe with anthropogenic warming. *Nature climate change*, *11*(6), 485-491. https://doi.org/10.1038/s41558-021-01044-3

Newman, M., & Sardeshmukh, P. D. (1998). The impact of the annual cycle on the North Pacific/North American response to remote low-frequency forcing. *Journal of the atmospheric sciences*, *55*(8), 1336-1353. https://doi.org/10.1175/1520-0469(1998)055<1336:TIOTAC>2.0.CO

2

Nguyen, N. M., & Choi, M. (2024). Delving into flash droughts in Vietnam during the last two decades using the standardized evaporative stress ratio. *Journal of hydrology (Amsterdam)*, *630*, 130669. https://doi.org/10.1016/j.jhydrol.2024.130669

Noguera, I., Domínguez-Castro, F., & Vicente-Serrano, S. M. (2020). Characteristics and trends of flash droughts in Spain, 1961–2018. *Annals of the New York Academy of Sciences*, *1472*(1), 155-172. https://doi.org/10.1111/nyas.14365

Oki, T., & Kanae, S. (2006). Global Hydrological Cycles and World Water Resources. *Science (American Association for the Advancement of Science)*, *313*(5790), 1068-1072. https://doi.org/10.1126/science.1128845

Orth, R., O, S., Zscheischler, J., Mahecha, M. D., & Reichstein, M. (2022). Contrasting biophysical and societal impacts of hydro-meteorological extremes. *Environmental research letters*, *17*(1), 014044. https://doi.org/10.1088/1748-9326/ac4139

Osman, M., Zaitchik, B. F., Badr, H. S., Otkin, J., Zhong, Y., Lorenz, D., . . . Holmes, T. (2022). Diagnostic Classification of Flash Drought Events Reveals Distinct Classes of Forcings and Impacts. *Journal of hydrometeorology*, *23*(2), 275-289. https://doi.org/10.1175/JHM-D-21-0134.1

Otkin, J. A., Anderson, M. C., Hain, C., & Svoboda, M. (2014). Examining the Relationship between Drought Development and Rapid Changes in the Evaporative Stress Index. *Journal of hydrometeorology*, *15*(3), 938-956. https://doi.org/10.1175/JHM-D-13-0110.1

Otkin, J. A., Anderson, M. C., Hain, C., Svoboda, M., Johnson, D., Mueller, R., . . . Brown, J. (2016). Assessing the evolution of soil moisture and vegetation conditions during the 2012 United States flash drought. *Agricultural and forest meteorology*, *218-219*, 230-242. https://doi.org/10.1016/j.agrformet.2015.12.065

Otkin, J. A., Haigh, T., Mucia, A., Anderson, M., & Hain, C. (2018). Comparison of Agricultural Stakeholder Survey Results and Drought Monitoring Datasets during the 2016 U.S. Northern Plains Flash Drought. *Weather, climate, and society*, *10*(4), 867-883. https://doi.org/10.1175/WCAS-D-18-0051.1

Otkin, J. A., Svoboda, M., Hunt, E. D., Ford, T. W., Anderson, M. C., Hain, C., & Basara, J. B. (2018). FLASH DROUGHTS: A Review and Assessment of the Challenges Imposed by Rapid-Onset Droughts in the United States. *Bulletin of the American Meteorological Society*, *99*(5), 911-920. https://doi.org/10.1175/BAMS-D-17-0149.1

Otkin, J. A., Woloszyn, M., Wang, H., Svoboda, M., Skumanich, M., Pulwarty, R., . . . Cravens, A. E. (2022). Getting ahead of Flash Drought: From Early Warning to Early Action. *Bulletin of the American Meteorological Society*, *103*(10), E2188-E2202. https://doi.org/10.1175/BAMS-D-21-0288.1

Otkin, J. A., Zhong, Y., Hunt, E. D., Basara, J., Svoboda, M., Anderson, M. C., & Hain, C. (2019). Assessing the Evolution of Soil Moisture and Vegetation Conditions during a Flash Drought–Flash Recovery Sequence over the South-Central United States. *Journal of hydrometeorology*, *20*(3), 549-562. https://doi.org/10.1175/JHM-D-18-0171.1

PaiMazumder, D., & Done, J. M. (2016). Potential predictability sources of the 2012 U.S. drought in observations and a regional model ensemble. *Journal of geophysical research. Atmospheres*, *121*(21), 12,581-512,592. https://doi.org/10.1002/2016JD025322

Palmer, W. C. (1965). Meteorological drought / Wayne C. Palmer.

Parker, T., Gallant, A., Hobbins, M., & Hoffmann, D. (2021). Flash drought in Australia and its relationship to evaporative demand. *Environmental research letters*, *16*(6), 64033. https://doi.org/10.1088/1748-9326/abfe2c

Pendergrass, A. G., Meehl, G. A., Pulwarty, R., Hobbins, M., Hoell, A., AghaKouchak, A., . . . Woodhouse, C. A. (2020). Flash droughts present a new challenge for subseasonal-to-seasonal prediction. *Nature climate change*, *10*(3), 191-199. https://doi.org/10.1038/s41558-020-0709-0

Rakovec, O., Samaniego, L., Hari, V., Markonis, Y., Moravec, V., Thober, S., . . . Kumar, R. (2022). The 2018–2020 Multi-Year Drought Sets a New Benchmark in Europe. *Earth's future*, *10*(3), n/a. https://doi.org/10.1029/2021EF002394

Rasmusson, E. M., & Carpenter, T. H. (1982). Variations in Tropical Sea Surface Temperature and Surface Wind Fields Associated with the Southern Oscillation/El Niño. *Monthly weather review*, *110*(5), 354-384. https://doi.org/10.1175/1520-0493(1982)110<0354:VITSST>2.0.CO

2

Reif, D. W., & Bluestein, H. B. (2017). A 20-Year Climatology of Nocturnal Convection Initiation over the Central and Southern Great Plains during the Warm Season. *Monthly weather review*, *145*(5), 1615-1639. https://doi.org/10.1175/MWR-D-16-0340.1

Rex, D. F. (1950). Blocking Action in the Middle Troposphere and its Effect upon Regional Climate: I. An Aerological Study of Blocking Action. *Tellus*, *2*(3), 196-211. https://doi.org/10.3402/tellusa.v2i3.8546

Russo, S., Dosio, A., Graversen, R. G., Sillmann, J., Carrao, H., Dunbar, M. B., . . . Vogt, J. V. (2014). Magnitude of extreme heat waves in present climate and their projection in a warming world. *Journal of geophysical research. Atmospheres*, *119*(22), 12,500-512,512. https://doi.org/10.1002/2014JD022098

Samaniego, L., Thober, S., Kumar, R., Wanders, N., Rakovec, O., Pan, M., . . . Landscape functioning, G. a. H. (2018). Anthropogenic warming exacerbates European soil moisture droughts. *Nature climate change*, *8*(5), 421-426. https://doi.org/10.1038/s41558-018-0138-5

Seager, R., & Henderson, N. (2016). On the Role of Tropical Ocean Forcing of the Persistent North American West Coast Ridge of Winter 2013/14a. *Journal of climate*, *29*(22), 8027-8049. https://doi.org/10.1175/JCLI-D-16-0145.1

Seager, R., Hoerling, M., Schubert, S., Wang, H., Lyon, B., Kumar, A., . . . Henderson, N. (2015). Causes of the 2011–14 California Drought. *Journal of climate*, *28*(18), 6997-7024. https://doi.org/10.1175/JCLI-D-14-00860.1

Sehgal, V., Gaur, N., & Mohanty, B. P. (2021). Global Flash Drought Monitoring Using Surface Soil Moisture. *Water resources research*, *57*(9), n/a. https://doi.org/10.1029/2021WR029901

Seneviratne, S. I., Corti, T., Davin, E. L., Hirschi, M., Jaeger, E. B., Lehner, I., . . . Teuling, A. J. (2010). Investigating soil moisture–climate interactions in a changing climate: A review. *Earth-science reviews*, *99*(3), 125-161. https://doi.org/10.1016/j.earscirev.2010.02.004

Seneviratne, S. I., Koster, R. D., Guo, Z., Dirmeyer, P. A., Kowalczyk, E., Lawrence, D., . . . Verseghy, D. (2006). Soil Moisture Memory in AGCM Simulations: Analysis of Global Land–Atmosphere Coupling Experiment (GLACE) Data. *Journal of hydrometeorology*, *7*(5), 1090-1112. https://doi.org/10.1175/JHM533.1

Shah, J., Hari, V., Rakovec, O., Markonis, Y., Samaniego, L., Mishra, V., . . . Kumar, R. (2022). Increasing footprint of climate warming on flash droughts occurrence in Europe. *Environmental research letters*, *17*(6), 64017. https://doi.org/10.1088/1748-9326/ac6888

Singh, J., Ashfaq, M., Skinner, C. B., Anderson, W. B., Mishra, V., & Singh, D. (2022). Enhanced risk of concurrent regional droughts with increased ENSO variability and warming. *Nature climate change*, *12*(2), 163-170. https://doi.org/10.1038/s41558-021-01276-3

Singh, J., Ashfaq, M., Skinner, C. B., Anderson, W. B., & Singh, D. (2021). Amplified risk of spatially compounding droughts during co-occurrences of modes of natural ocean variability. *NPJ climate and atmospheric science*, *4*(1), 1-14. https://doi.org/10.1038/s41612-021-00161-2

Spinoni, J., Barbosa, P., De Jager, A., McCormick, N., Naumann, G., Vogt, J. V., . . . Mazzeschi, M. (2019). A new global database of meteorological drought events from 1951 to 2016. *Journal of hydrology. Regional studies*, *22*, 100593. https://doi.org/10.1016/j.ejrh.2019.100593

Stagge, J. H., Kohn, I., Tallaksen, L. M., & Stahl, K. (2015). Modeling drought impact occurrence based on meteorological drought indices in Europe. *Journal of hydrology (Amsterdam)*, *530*, 37-50. https://doi.org/10.1016/j.jhydrol.2015.09.039

Stocker, B. D., Zscheischler, J., Keenan, T. F., Prentice, I. C., Seneviratne, S. I., & Peñuelas, J. (2019). Drought impacts on terrestrial primary production underestimated by satellite monitoring. *Nature geoscience*, *12*(4), 264-270. https://doi.org/10.1038/s41561-019-0318-6

Stéfanon, M., Drobinski, P., D'Andrea, F., & de Noblet-Ducoudré, N. (2012). Effects of interactive vegetation phenology on the 2003 summer heat waves: EFFECTS OF PHENOLOGY ON HEAT WAVES. *Journal of Geophysical Research: Atmospheres*, *117*(D24), n/a. https://doi.org/10.1029/2012JD018187

Svoboda, M., LeComte, D., Hayes, M., Heim, R., Gleason, K., Angel, J., . . . Stephens, S. (2002). THE DROUGHT MONITOR. *Bulletin of the American Meteorological Society*, *83*(8), 1181-1190. https://doi.org/10.1175/1520-0477-83.8.1181

Swain, D. L., Singh, D., Horton, D. E., Mankin, J. S., Ballard, T. C., & Diffenbaugh, N. S. (2017). Remote Linkages to Anomalous Winter Atmospheric Ridging Over the Northeastern Pacific. *Journal of geophysical research. Atmospheres*, *122*(22), 12,194-112,209. https://doi.org/10.1002/2017JD026575

Tian, L., Yuan, S., & Quiring, S. M. (2018). Evaluation of six indices for monitoring agricultural drought in the south-central United States. *Agricultural and forest meteorology*, *249*, 107-119. https://doi.org/10.1016/j.agrformet.2017.11.024

Vogel, M. M., Zscheischler, J., & Seneviratne, S. I. (2018). Varying soil moisture–atmosphere feedbacks explain divergent temperature extremes and precipitation projections in central Europe. *Earth system dynamics*, *9*(3), 1107-1125. https://doi.org/10.5194/esd-9-1107-2018

Wada, Y., van Beek, L. P. H., Wanders, N., & Bierkens, M. F. P. (2013). Human water consumption intensifies hydrological drought worldwide. *Environmental research letters*, *8*(3), 34036. https://doi.org/10.1088/1748-9326/8/3/034036

Wen, J., Hua, Y., Cai, C., Wang, S., Wang, H., Zhou, X., . . . Wang, J. (2023). Probabilistic Forecast and Risk Assessment of Flash Droughts Based on Numeric Weather Forecast: A Case Study in Zhejiang, China. *Sustainability (Basel, Switzerland)*, *15*(4), 3865. https://doi.org/10.3390/su15043865

Weyn, J. A., Durran, D. R., Caruana, R., & Cresswell-Clay, N. (2021). Sub-Seasonal Forecasting With a Large Ensemble of Deep-Learning Weather Prediction Models. *Journal of advances in modeling earth systems*, *13*(7), n/a. https://doi.org/10.1029/2021MS002502

Wilhite, D. A., & Glantz, M. H. (1985). Understanding: the Drought Phenomenon: The Role of Definitions. *Water international*, *10*(3), 111-120. https://doi.org/10.1080/02508068508686328

Wilhite, D. A., Svoboda, M. D., & Hayes, M. J. (2007). Understanding the complex impacts of drought: A key to enhancing drought mitigation and preparedness. *Water resources management*, *21*(5), 763-774. https://doi.org/10.1007/s11269-006-9076-5

Yao, T., Liu, S., Hu, S., & Mo, X. (2022). Response of vegetation ecosystems to flash drought with solar-induced chlorophyll fluorescence over the Hai River Basin, China during 2001–

2019. *Journal of environmental management*, *313*, 114947-114947. https://doi.org/10.1016/j.jenvman.2022.114947

Yuan, X., Wang, L., Wu, P., Ji, P., Sheffield, J., & Zhang, M. (2019). Anthropogenic shift towards higher risk of flash drought over China. *Nature communications*, *10*(1), 4661-4668. https://doi.org/10.1038/s41467-019-12692-7

Yuan, X., Wang, Y., Ji, P., Wu, P., Sheffield, J., & Otkin, J. A. (2023). A global transition to flash droughts under climate change. *Science (American Association for the Advancement of Science)*, *380*(6641), 187-191. https://doi.org/10.1126/science.abn6301

Zaitchik, B. F., Macalady, A. K., Bonneau, L. R., & Smith, R. B. (2006). Europe's 2003 heat wave: a satellite view of impacts and land–atmosphere feedbacks. *International journal of climatology*, *26*(6), 743-769. https://doi.org/10.1002/joc.1280

Zhang, J., Campana, P. E., Yao, T., Zhang, Y., Lundblad, A., Melton, F., & Yan, J. (2018). The water-food-energy nexus optimization approach to combat agricultural drought: a case study in the United States. *Applied energy*, *227*, 449-464. https://doi.org/10.1016/j.apenergy.2017.07.036

Zhang, X., Liu, Y., Zhu, Y., Ma, Q., Philippe, G., Qu, Y., & Yin, H. (2023). Probabilistic analysis on the influences of heatwaves during the onset of flash droughts over China. *Hydrology Research*, *54*(7), 869-884. https://doi.org/10.2166/nh.2023.022

Zhao, M., Zhang, H., & Dharssi, I. (2019). On the soil moisture memory and influence on coupled seasonal forecasts over Australia. *Climate dynamics*, *52*(11), 7085-7109. https://doi.org/10.1007/s00382-018-4566-8